Data analysis for RT-PCR

We used the LightCycler Software version 3.5 program (Roche Molecular Biochemicals, Basel, Switzerland) to calculate the cycle numbers. After proportional baseline adjustment, a fit point method was used to determine the cycle in which the log-linear signal was first distinguishable from the baseline. This cycle number was used as the crossing point value. A standard curve was produced by measuring the crossing point of each standard value and plotting it against the logarithmic value of the concentration. Concentrations of unknown samples were calculated by plotting their crossing points against the standard curve and dividing by *GAPDH* content. The results of RT-PCR were sent from Beppu to Tokyo for analyses.

Immunohistochemistry

Immunohistochemistry was performed on paraffin-embedded specimens obtained from patients with metastatic gastric cancer and two healthy volunteers. Tissue sections were deparaffinised, soaked in 0.01 M sodium citrate buffer and boiled in a microwave for 5 min at 500 W to retrieve cell antigens. The primary rabbit polyclonal antibody against ID1 (C-20; Santa Cruz Biotechnology, Santa Cruz, CA, USA), which detects ID1 in paraffin-embedded human tissue sections and does not crossreact with ID2, ID3 or ID4 (Maruyama *et al*, 1999), was used at a dilution of 1 : 100. The blocking peptide to ID1 (sc-488P, Santa Cruz Biotechnology) was used as a negative control (Supplementary Figure 4). Tissue sections were immunohistochemically stained using the avidin-biotin-peroxidase method (LSAB+ system-HRP; DAKO, Kyoto, Japan). All sections were counterstained with haematoxylin.

Statistical analysis

The expression of *ID1* was adjusted in each case for *GAPDH* expression. For continuous variables, data were expressed as the means ± s.d. The relationship between *ID1* mRNA expression and clinicopathlogical factors was analysed using a χ^2 test and Student's *t*-test. All tests were analysed using JMP software (SAS Institute Inc., Cary, NC, USA) and the findings were considered significant when the *P*-value was <0.05.

RESULTS

Expression of *ID1* mRNA in bone marrow of gastric cancer

Figure 1A shows expression of *ID1* mRNA in bone marrow according to staging classification. In bone marrow, the mean expression level of *ID1* mRNA in stage IV (957 ± 169) was significantly higher than other stages ($P=0.003$). Specifically, the levels of stages I, II and III were 54 ± 185, 472 ± 208, and 767 ± 205, respectively. To confirm the specificity of *ID1*, we performed RT-PCR analysis of six representative cases in each stage, which was very close to the average value (Figure 1C). In addition, sequencing of these transcripts confirmed that it was the product of *ID1* (Supplementary Figure 1).

Expression of *ID1* mRNA in peripheral blood of gastric cancer

In the peripheral blood samples, there was a significant relationship between the expression level of *ID1* mRNA and the progression of gastric cancer cases (Figure 1B). The mean expression level of *ID1* mRNA in stage IV (105 ± 15) was significantly higher ($P=0.0001$) than stages I, II and III (12.4 ± 15.4, 29.6 ± 15.5, and 38.3 ± 16.0, respectively). In addition, there was a significant correlation between the expression of *ID1* mRNA in bone marrow and peripheral blood ($r=0.23$, $P=0.002$, data not shown).

ID1 expression and clinicopathological features of gastric cancer patients

We examined the clinicopathlogical significance of *ID1* mRNA in samples from bone marrow and peripheral blood (Table 1). In both bone marrow and peripheral blood, there are significant associations with many cliniopathlogical features such as tumour size and depth of tumour invasion. Especially, in patients with evidence of lymphatic invasion, lymph node metastasis or peritoneal dissemination, we found significantly higher expression of *ID1* mRNA in bone marrow samples compared to patients without metastasis. ($P=0.001$, $P=0.001$ and $P=0.002$, respectively, Figures 2A-C). Similarly, in peripheral blood samples, the cases with lymphatic invasion, lymph node metastasis or peritoneal dissemination had significantly higher expression of *ID1* mRNA compared to patients without metastasis. ($P=0.02$, $P=0.02$ and $P<0.0001$ respectively, Figures 3A-C).

Expression of ID1 protein in bone marrow from patients with metastatic gastric cancer and healthy volunteers

The ID1 protein expression in bone marrow was evaluated immunohistochemically in studies of metastatic gastric cancer patients and healthy volunteers. In bone marrow of healthy volunteer (Figure 4A), the ID1 expression was localised mainly in the nuclei of bone marrow cells. The population of ID1-positive cells in healthy volunteer is lower than that in metastatic patient (Figure 4B). The ID1 expression of bone marrow cells with metastatic patient was also localised mainly in the nuclei. We also examined the ID1 expression of bone marrow carcinomatosis resulting from gastric cancer. The metastasized cancer cells were confirmed to be epithelial cells by HE (Supplementary Figure 2A) stain and AE1/AE3 (Supplementary Figure 2B). These cells were stained slightly with ID1 antibody in the cytoplasm (Figure 4C).

ID1 expression in primary lesions and metastatic lesions of gastric cancer

We examined the ID1 protein expression immunohistochemically in 30 primary lesions, 3 metastatic lymph nodes and 3 peritoneal disseminated lesions of gastric cancer cases. We found that 20 cases have high ID1 expression in primary lesions (Figure 5A). Some of the cases showed weak (Supplementary Figure 3A) or moderate (Supplementary Figure 3B) ID1 staining. In addition, two of three metastatic lymph nodes and peritoneal disseminated lesions were stained slightly with the ID1 antibody and the ID1 expression was localised in the cytoplasm of cancer cells in primary lesion, metastatic lymph node metastasis and peritoneal dissemination (Figures 5B and C).

DISCUSSION

Peritoneal dissemination is recognised as the most critical factor in assessing the prognosis of gastric cancer cases (Bando *et al*, 1999). There is no conclusive evidence, however, whether peritoneal dissemination might be established by the lymph node metastasis as well as direct dissemination from the serosal layer of stomach (Yonemura *et al*, 2007). In this study, the *ID1* mRNA expression in bone marrow and peripheral blood was significantly associated with lymph node metastasis and peritoneal dissemination. Therefore, we suggest that peritoneal dissemination of gastric cancer is mediated through lymph node metastasis combined with the *ID1*-expressing endothelial cells from bone marrow. From a clinical point of view, there are no convincing markers for

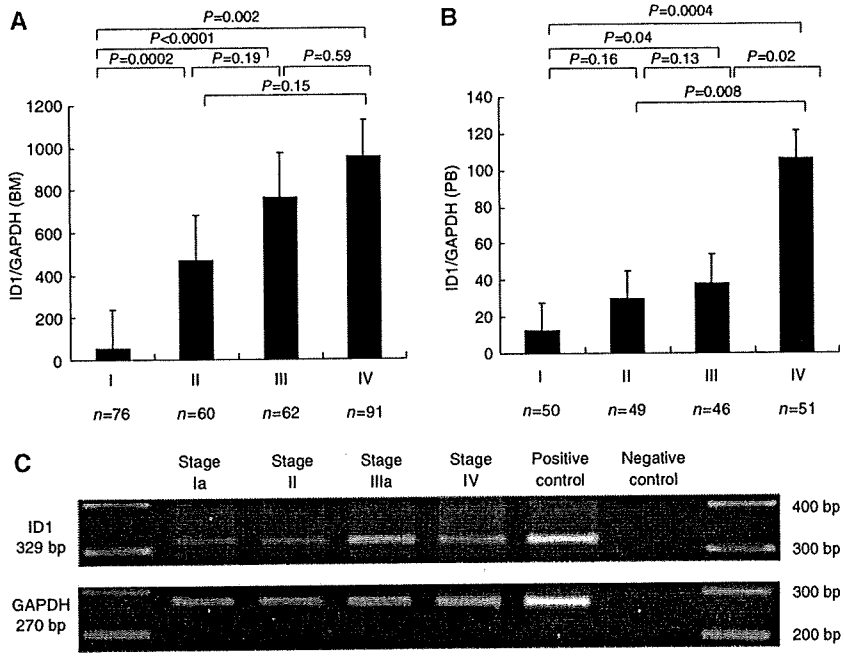

Figure 1 The mean value of *ID1* mRNA expression normalised *GAPDH* in bone marrow (**A**) and peripheral blood (**B**) according to staging classification. Group stage I consisted of patients with tumours that invaded less than the sub-mucosal layer and no lymph node metastasis (BM: $n=76$; PB: $n=50$). Group stage II consisted of patients with tumours that penetrated serosa or lymph node metastasis (Group 1) (BM: $n=60$; PB: $n=49$). Group stage III consisted of patients with tumours invasion of adjacent structures or lymph node metastasis (Group 2 or 3) (BM: $n=62$; PB: $n=46$). Group stage IV consisted of patients with distant metastasis (BM: $n=91$; PB: $n=51$). The mean value of *ID1* mRNA expression in bone marrow and peripheral blood increased along with the progression of stage. The RT–PCR analysis of four representative bone marrow samples was performed in each stage (**C**: upper, *ID1* product size 329 bp, lower, *GAPDH* product size 270 bp).

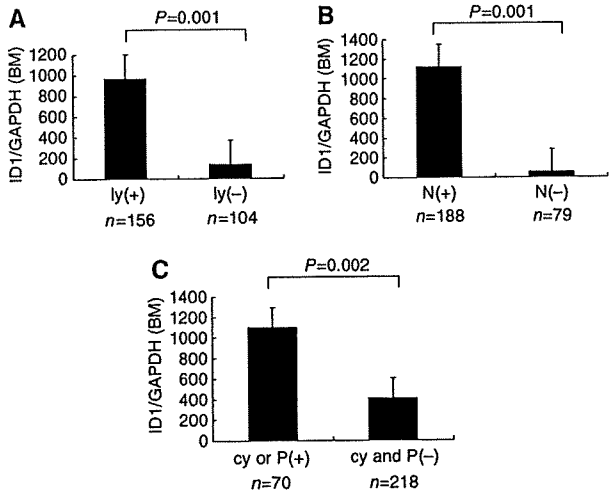

Figure 2 Comparison of the *ID1* mRNA expression in bone marrow of patients with or without lymphatic invasion (ly) (+: $n=156$, −: $n=104$; **A**), lymph node metastasis (*N*) (+: $n=188$, −: $n=79$; **B**) and peritoneal cytology (cy) or peritoneal metastasis (P) (+: $n=70$; −: $n=218$; **C**). In patients with evidence of lymphatic invasion, lymph node metastasis or peritoneal dissemination, the expression of *ID1* mRNA in bone marrow was significantly higher compared to patients without metastasis.

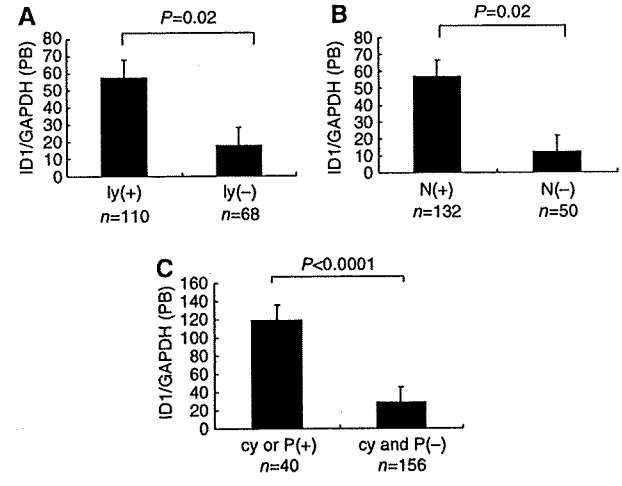

Figure 3 Comparison of the *ID1* mRNA expression in peripheral blood of patients with or without lymphatic invasion (ly) (+: $n=110$, −: $n=68$; **A**), lymph node metastasis (N) (+: $n=132$, -: $n=50$; **B**) and peritoneal cytology (cy) or peritoneal metastasis (P) (+: $n=40$, −: $n=156$; **C**). In patients with evidence of lymphatic invasion, lymph node metastasis or peritoneal dissemination, the expression of *ID1* mRNA in peripheral blood was significantly higher compared to patients without metastasis.

peritoneal dissemination before surgery. Therefore, it is significant that the *ID1* expression in bone marrow and peripheral blood can be used as a reliable marker before surgery to determine which gastric cancer patients are likely to have peritoneal dissemination mediated through lymph node metastasis.

There are two possible sources of the *ID1*-positive cells: ITC and host cells (such as EPCs, as stated by Gao *et al*). With regard to tumour cells, Tsuchiya *et al* showed that the number and size of

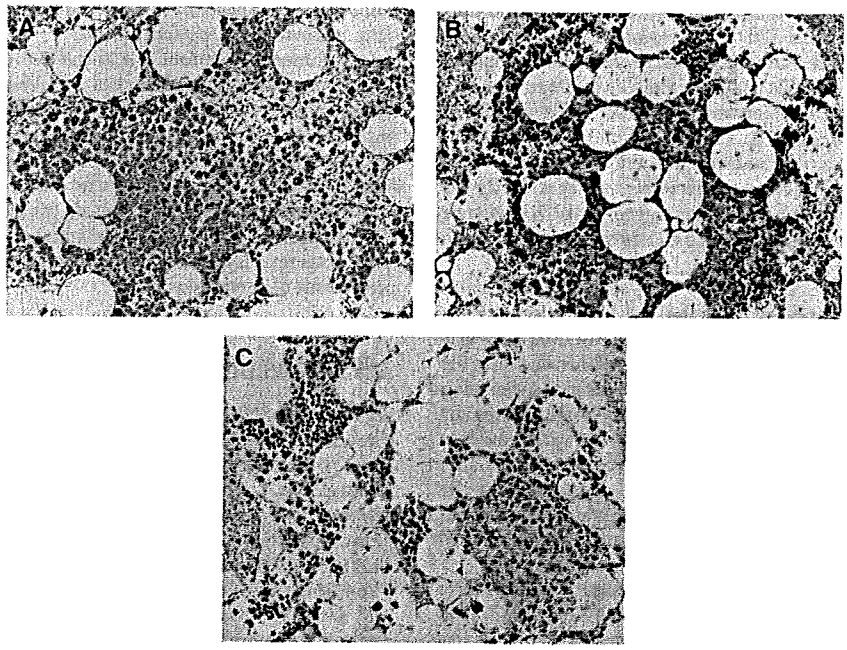

Figure 4 Immunohistochemistry with ID1 antibody, assessing bone marrow from a representative healthy volunteer and metastatic gastric cancer patient. In the bone marrow of healthy volunteer (**A**), the ID1 expression was localised mainly in the nuclei of bone marrow cells. The population of ID1-positive cells in healthy volunteer is lower than that in metastatic patients (**B**). The metastasized cells confirmed to be epithelial cells by HE stain and AE1/AE3 (Supplementary Figures 2A and B) that originated from gastric cancer were stained slightly with ID1 in cytoplasm (**C**). (**A**–**C**: original magnification: × 100).

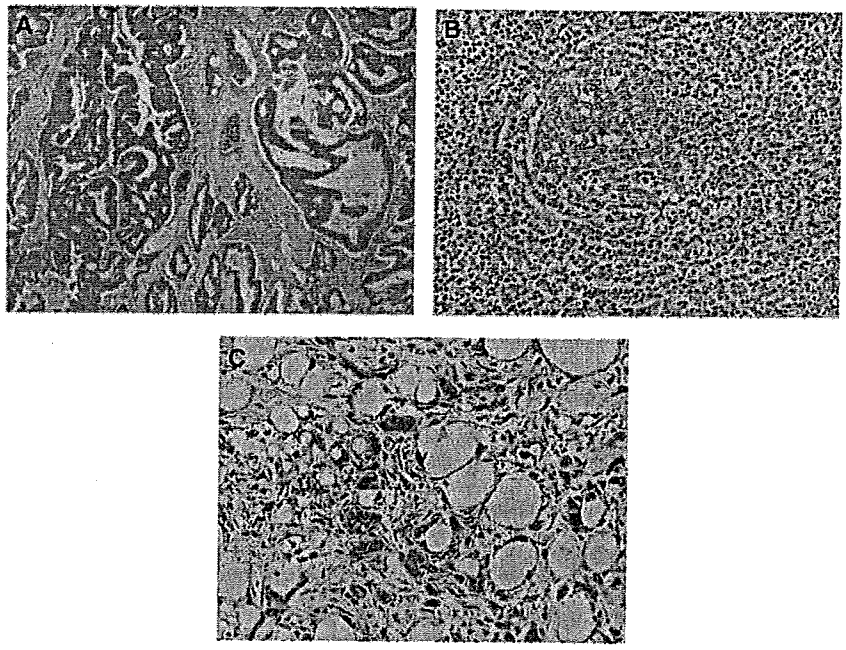

Figure 5 Immunohistochemistry with ID1 antibody assessing primary and metastatic lesions. Most of the primary lesions of gastric cancer were stained strongly with the ID1 antibody. A representative case was shown in (**A**). The ID1 expression was localised in the cytoplasm of cancer cells in primary lesion, metastatic lymph node metastasis (**B**) and peritoneal dissemination (**C**). (Original magnification: **A**: × 40, **B** and **C**: × 100).

peritoneal metastatic nodules formed by ID1 and ID3 double-knockdown gastric cancer cells were reduced in comparison to mock-transfected control cells *in vivo* (Tsuchiya *et al*, 2005). Furthermore, Kim *et al* reported that transgenic mice expressing a thymocyte-specific Id1 gene developed T-cell lymphoma *in vivo* (Kim *et al*, 1999). In addition, overexpression of ID1 in the primary cancer cells relative to normal mucosa has been observed in primary human oesophageal (Hu *et al*, 2001) and colorectal cancers (Wilson *et al*, 2001). Those reports found that the ID1 expression was significantly associated with the differentiation of

cells and a poor prognosis. In gastric cancer, Han *et al* found that strong immunohistochemical ID1 expression was associated with poorer differentiation and more aggressive behaviour of tumour cells (Han *et al*, 2004). In this study, we also examined the ID1 expression in primary lesion of gastric cancer cases. We found that two-thirds cases have high ID1 expression in primary lesions (Figure 5A). Furthermore, we showed that the metastasized cancer cells from gastric cancer in bone marrow were slightly stained with ID1 antibody (Figure 4C). These findings suggest that *ID1* may be a potential oncogene. As for the origin of ID1-positive cells in bone marrow, these seem to represent ITCs.

On the other hand, in this study, we present two lines of evidence indicating that the origin of the ID1 expression is from host cells, perhaps originating from bone marrow or peripheral blood. First, immunohistochemical studies showed that the population of ID1-positive cells in healthy volunteer is lower than that in metastatic patients (Figure 4A). Thus, ID1-expressing cells are particularly numerous in the bone marrow in which there are relatively few cancer cells. The current findings may suggest that ID1 is not a component of the aggregated cancer cells in the metastatic lymph nodes and peritoneal disseminated tumours, but instead plays a supportive role for gastric cancer cells to form lymph node metastasis and peritoneal dissemination.

Secondary, Gao *et al* found that Id1 was expressed by EPC positive for VE-cadherin and CD31 in peripheral blood (Gao *et al*, 2008). As we expected, the *ID1* expression in peripheral blood was significantly related to the incidence of peritoneal dissemination. In addition, there were significant association between *ID1* expression in peripheral blood and those in bone marrow from gastric cancer cases. This finding may indicate that the expression of *ID1* in peripheral blood originates from the circulating progenitor cells (CPCs), including EPC and from the bone marrow (Lyden *et al*, 2001). Those results may suggest that the origin of *ID1* expression is not only from cancer cells but also from host cells, such as CPCs in bone marrow and peripheral blood.

In summary, we found that the *ID1* mRNA expression in bone marrow and peripheral blood is a reliable predictive marker for lymph node metastasis and peritoneal dissemination, which indicates a poor prognostic outlook in gastric cancer. In addition, our findings suggest that the *ID1* expression originates from not only the cancer cells but also the host side progenitor cells with the cancer-bearing condition. Therefore, we propose that targeting the *ID1*-expressing cells in the bone marrow and/or peripheral blood after surgery represents a new concept for the treatment and/or prevention of metastasis.

ACKNOWLEDGEMENTS

We thank T Shimooka, K Ogata, M Kasagi, Y Nakagawa and T Kawano for their technical assistance. This work was supported in part by the following grants and foundations: CREST, Japan Science and Technology Agency (JST); Japan Society for the Promotion of Science (JSPS) Grant-in-Aid for Scientific Research, grant numbers 17109013, 18659384, 18390367, 18590333, 18015039, 19591509, 19390336, 20390360, 20591547, 20790961 and 20790960; The Ministry of Education, Culture, Sports, Science and Technology (MEXT) Grant-in-Aid for Scientific Research on Priority Areas, grant number 18015039; Third Term Comprehensive Ten-year Strategy for Cancer Control, grant number 16271201; NEDO (New Energy and Industrial Technology Development Organization) Technological Development for Chromosome Analysis.

Supplementary Information accompanies the paper on British Journal of Cancer website (http://www.nature.com/bjc)

REFERENCES

Bando E, Yonemura Y, Takeshita Y, Taniguchi K, Yasui T, Yoshimitsu Y, Fushida S, Fujimura T, Nishimura G, Miwa K (1999) Intraoperative lavage for cytological examination in 1297 patients with gastric carcinoma. *Am J Surg* 178: 256–262

Benezra R, Davis RL, Lockshon D, Turner DL, Weintraub H (1990) The protein Id: a negative regulator of helix-loop-helix DNA binding proteins. *Cell* 61: 49–59

Fong S, Itahana Y, Sumida T, Singh J, Coppe JP, Liu Y, Richards PC, Bennington JL, Lee NM, Debs RJ, Desprez PY (2003) Id-1 as a molecular target in therapy for breast cancer cell invasion and metastasis. *Proc Natl Acad Sci USA* 100: 13543–13548

Gao D, Nolan DJ, Mellick AS, Bambino K, McDonnell K, Mittal V (2008) Endothelial progenitor cells control the angiogenic switch in mouse lung metastasis. *Science* 319: 195–198

Han S, Gou C, Hong L, Liu J, ZheyiHan Liu C, Wang J, Wu K, Ding J, Fan D (2004) Expression and significances of Id1 helix-loop-helix protein overexpression in gastric cancer. *Cancer Lett* 216: 63–71

Hu YC, Lam KY, Law S, Wong J, Srivastava G (2001) Identification of differentially expressed genes in esophageal squamous cell carcinoma (ESCC) by cDNA expression array: overexpression of Fra-1, Neogenin, Id-1, and CDC25B genes in ESCC. *Clin Cancer Res* 7: 2213–2221

Iinuma H, Okinaga K, Egami H, Mimori K, Hayashi N, Nishida K, Adachi M, Mori M, Sasako M (2006) Usefulness and clinical significance of quantitative real-time RT-PCR to detect isolated tumor cells in the peripheral blood and tumor drainage blood of patients with colorectal cancer. *Int J Oncol* 28: 297–306

Kaplan RN, Riba RD, Zacharoulis S, Bramley AH, Vincent L, Costa C, MacDonald DD, Jin DK, Shido K, Kerns SA, Zhu Z, Hicklin D, Wu Y, Port JL, Altorki N, Port ER, Ruggero D, Shmelkov SV, Jensen KK, Rafii S, Lyden D (2005) VEGFR1-positive haematopoietic bone marrow progenitors initiate the pre-metastatic niche. *Nature* 438: 820–827

Kim D, Peng XC, Sun XH (1999) Massive apoptosis of thymocytes in T-cell-deficient Id1 transgenic mice. *Mol Cell Biol* 19: 8240–8253

Lyden D, Hattori K, Dias S, Costa C, Blaikie P, Butros L, Chadburn A, Heissig B, Marks W, Witte L, Wu Y, Hicklin D, Zhu Z, Hackett NR, Crystal RG, Moore MA, Hajjar KA, Manova K, Benezra R, Rafii S (2001) Impaired recruitment of bone-marrow-derived endothelial and hematopoietic precursor cells blocks tumor angiogenesis and growth. *Nat Med* 7: 1194–1201

Maruyama H, Kleeff J, Wildi S, Friess H, Buchler MW, Israel MA, Korc M (1999) Id-1 and Id-2 are overexpressed in pancreatic cancer and in dysplastic lesions in chronic pancreatitis. *Am J Pathol* 155: 815–822

Maruyama K, Kaminishi M, Hayashi K, Isobe Y, Honda I, Katai H, Arai K, Kodera Y, Nashimoto A (2006) Gastric cancer treated in 1991 in Japan: data analysis of nationwide registry. *Gastric Cancer* 9: 51–66

Mimori K, Fukagawa T, Kosaka Y, Kita Y, Ishikawa K, Etoh T, Iinuma H, Sasako M, Mori M (2008) Hematogenous metastasis in gastric cancer requires isolated tumor cells and expression of vascular endothelial growth factor receptor-1. *Clin Cancer Res* 14: 2609–2616

Mori M, Mimori K, Inoue H, Barnard GF, Tsuji K, Nanbara S, Ueo H, Akiyoshi T (1995) Detection of cancer micrometastases in lymph nodes by reverse transcriptase-polymerase chain reaction. *Cancer Res* 55: 3417–3420

Ogawa K, Utsunomiya T, Mimori K, Tanaka F, Inoue H, Nagahara H, Murayama S, Mori M (2005) Clinical significance of human kallikrein gene 6 messenger RNA expression in colorectal cancer. *Clin Cancer Res* 11: 2889–2893

Tsuchiya T, Okaji Y, Tsuno NH, Sakurai D, Tsuchiya N, Kawai K, Yazawa K, Asakage M, Yamada J, Yoneyama S, Kitayama J, Osada T, Watanabe T, Tokunaga K, Takahashi K, Nagawa H (2005) Targeting Id1 and Id3 inhibits peritoneal metastasis of gastric cancer. *Cancer Sci* 96: 784–790

Wilson JW, Deed RW, Inoue T, Balzi M, Becciolini A, Faraoni P, Potten CS, Norton JD (2001) Expression of Id helix-loop-helix proteins in colorectal adenocarcinoma correlates with p53 expression and mitotic index. *Cancer Res* 61: 8803–8810

Yonemura Y, Endo Y, Obata T, Sasaki T (2007) Recent advances in the treatment of peritoneal dissemination of gastrointestinal cancers by nucleoside antimetabolites. *Cancer Sci* 98: 11–18

British Journal of Cancer (2009) 100, 153–159

www.bjcancer.com

Expression of *uPAR* mRNA in peripheral blood is a favourite marker for metastasis in gastric cancer cases

Y Kita[1,2], T Fukagawa[3], K Mimori[1], Y Kosaka[1], K Ishikawa[1], T Aikou[2], S Natsugoe[2], M Sasako[3] and M Mori*[,1]

[1]Department of Surgery, Medical Institute of Bioregulation, Kyushu University, 4546, Tsurumihara, Beppu 874-0838, Japan; [2]Department of Surgical Oncology and Digestive Surgery, Field of Oncology, Course of Advanced Therapeutics, Kagoshima University, Graduate School of Medical and Dental Science, Kagoshima University, 8-35-1, Sakuragaoka, Kagoshima 890-8520, Japan; [3]Gastric Surgery Division, National Cancer Center Hospital, 5-1-1 Tsukiji, Chuo-ku 104-0045, Japan

Urokinase-type plasminogen activator receptor (*uPAR*) plays a central role in the plasminogen activation cascade and participates in extracellular matrix degradation, cell migration and invasion. We evaluated the expression level of *uPAR* mRNA and the presence of isolated tumour cells (ITCs) in bone marrow (BM) and peripheral blood (PB) in gastric cancer patients and clarified its clinical significance. We assessed specific *uPAR* mRNA expression by quantitative real-time reverse transcriptase- polymerase chain reaction (RT–PCR) in BM and PB in 846 gastric cancer patients as well as three epithelial cell markers, carcinoembryonic antigen (*CEA*), cytokeratin *(CK)-19* and *CK-7*. The *uPAR* mRNA expression in bone marrow and peripheral blood expressed significantly higher than normal controls ($P<0.0001$). The *uPAR* mRNA in BM showed concordant expression with the depth of tumour invasion, distant metastasis, and the postoperative recurrence ($P=0.015$, 0.044 and 0.010, respectively); whereas in PB, we observed more intimate significant association between *uPAR* expression and clinicopathologic variables, such as depth of tumour invasion, the distant metastasis, the venous invasion and the clinical stage ($P=0.009$, 0.002, 0.039 and 0.008, respectively). In addition, the *uPAR* mRNA expression in PB was an independent prognostic factor for distant metastasis by multivariate analysis. We disclosed that it was possible to identify high-risk patients for distant metastasis by measuring *uPAR* mRNA especially in peripheral blood at the timing of operation in gastric cancer patients.

British Journal of Cancer (2009) **100,** 153–159. doi:10.1038/sj.bjc.6604806 www.bjcancer.com
Published online 2 December 2008

Keywords: gastric cancer; circulating tumour cells; peripheral blood; bone marrow; urokinase-type plasminogen activator receptor (*uPAR*); metastasis

The presence of isolated tumour cells (ITCs) in bone marrow (BM) and peripheral blood (PB) is missed by conventional imaging system, and ITCs expected to be a determinant factor of subsequent formation of micrometastasis. The search for ITCs in patients with curatively resected tumours is of considerable importance, because early dissemination of tumour cells is one of the leading causes of relapse at the distant site and of death from cancer (Hellman, 1997). In spite of large number of studies to determine the clinicopathologic significance of ITCs in human solid carcinomas, much efforts have been made and found no definitive evidence to conclude these controversial issues, such as the way to identify ITCs and the appropriate biologic marker to predict the metastatic ability of gastric cancer cells (Heiss *et al*, 1995, 1997, 2002; Jauch *et al*, 1996; Hardingham *et al*, 2000; Lecomte *et al*, 2002; Natsugoe *et al*, 2003; Ikeguchi and Kaibara, 2005).

To identify ITCs in BM or PB, a bunch of molecular targets, such as CEA, CK7, CK18, CK18, CK19 and MAGE families have been applied and examined whether those genes were applicable to detect ITCs. Above all candidates, *CEA* and cytokeratin *(CK)*, epithelial cell surface markers were frequently used to be applied to detect ITCs instead of the direct detection of cancer cells in those ITC studies. However, our recent study disclosed that ITCs in BM and PB from gastric cancer could not be specified by the presence of CEA and/or CKs by RT-PCR, because those genes were detected ubiquitously among stages of 810 patients of gastric cancer. Therefore, we must identify a favourite marker to detect ITCs specifically as well as to predict metastasis precisely. In the current study, we focused on urokinase-type plasminogen activator receptor (*uPAR*) gene as a target molecule to detect isolated tumour cells in blood and bone marrow. This is because that in gastric cancer, several reports showed clearly that uPAR expression in bone marrow (BM) is one of the useful prognostic marker by immunohistochemistry (Heiss *et al*, 1995, 2002; Allgayer *et al*, 1997). However, there are no earlier reports of the clinical significance of the gene expression level of *uPAR* with quantitative RT-PCR assay that enabled us to examine objectively and repeatedly. Therefore, the aim of the current study was to evaluate the expressions of *uPAR* mRNA in bone marrow and peripheral blood in more than 800 cases of gastric cancer and to define its clinicopathologic and prognostic significance in gastric cancer patients.

*Correspondence: Dr M Mori;
E-mail: mmori@tsurumi.beppu.kyushu-u.ac.jp
Received 1 July 2008; revised 11 November 2008; accepted 11 November 2008; published online 2 December 2008

MATERIALS AND METHODS

Gastric cancer cases

A total of 846 gastric cancer patients who underwent surgical treatment in the National Cancer Center Hospital, Japan from 2001 to 2004 were studied. Clinical stages and pathological features of primary tumours were defined according to the classification of the International Union Against Cancer (Sobin and Fleming, 1997). There were 567 male and 279 female patients with average age 61.5, and a range of 27–87 years. None of these patients underwent endoscopic mucosal resection or palliative resection. Written informed consent had been obtained from all patients.

Normal controls

For normal negative controls, both peripheral blood and bone marrow were collected from 25 patients having no malignancy from April 2000 to March 2003. This group included 16 cases of gallstone, three cases of common bile duct stone, and six cases of incisional hernia. We extracted BM from the sternum of patients without malignancies but had operations under general anaesthesia.

Bone marrow and blood samples

Aspiration of both BM and PB was conducted immediately prior to operation under general anaesthesia. The aspirated BM was obtained from the sternum using a bone marrow aspiration needle (MDTECH, Gainesville, FL, USA). Peripheral blood was obtained through a venous catheter. The 1 ml of both BM and PB samples was discarded to avoid the contamination of the epidermal cells (Iinuma *et al*, 2006). Each 1 ml sample of BM and PB was immediately mixed with 4 ml of ISOGEN-LS (Nippon Gene, Toyama, Japan) and stored at −80°C until RNA extraction.

Total RNA extraction and first strand cDNA synthesis

Total RNA was according to the ISOGEN-LS manufacturer's protocols. All the clinical samples obtained in National Cancer Center Hospital were sent to our institute. The reverse transcriptase reaction (RT) was performed as described earlier (Mori *et al*, 1995; Masuda *et al*, 2002). The first strand cDNA was synthesized from 2.7 μg of total RNA in a 30 μl reaction mixture containing 5 μl 5 × RT reaction buffer (BRL, Gaithersburg, MD, USA), 200 μM dNTP, 100 μM solution of random hexadeoxynucleotide mixture, 50 units of Rnasin (Promega, Madison, WI, USA), 2 μl of 0.1 M dithiothreitol, and 100 U of Molony leukaemia virus RT (BRL). The mixture was incubated at 37°C for 60 min, heated to 95°C for 10 min, and then chilled on ice.

Primers and probes for detecting ITCs and *uPAR* expression

Quantitative RT–PCR methodology was designed to optimise the specificity and fidelity of the assay. The Kyushu University group had previously investigated the expression of seven representative molecular markers (carcinoembryonic antigen (*CEA*), *CK-7*, *CK-18*, *CK-19*, *CK-20*, mammaglobin and mucin (*MUC*)-1) in 27 cancers and eight non-epithelial cell lines using quantitative RT–PCR. The expression levels of *CK-7* and *CK-19* showed high sensitivity and specificity for the identification of gastric cancer cells in comparison with the other markers (Masuda *et al*, 2005). Those epithelial cell markers have been widely used as target genes for the detection of ITCs (Mori *et al*, 1996, 1998; Yamaguchi *et al*, 2000; Bessa *et al*, 2003; Sadahiro *et al*, 2005). Thus, *CEA*, *CK-7*, *CK-19* and *GAPDH* were studied by quantitative RT–PCR in all 846 patients (Mimori *et al*, 2008). Isolated tumour cells were considered to be 'present' when any single marker was positive. The reverse transcriptase reaction was performed as described elsewhere (Mimori *et al*, 2008). We performed real-time quantitative RT–PCR using a LightCycler instrument (Roche Diagnostics, Manheim, Germany) to detect ITCs in peripheral blood and/or bone marrow as the previous study.

Moreover, a *uPAR*-specific oligonucleotide primer was designed as follows: sense, 5′-TGAATCAATGTCTGGTAGC-3′ and antisense, 5′-TGGTTACAGCCACTTTTAGT-3′. The donor and acceptor probe sequences for *uPAR* identification were 5′-GCTATATGGTA AGAGGCTGTGCAACCGCCT-fluorescein and 5′-LC-Red640-AAT GTGCCAACATGCCCACCTGGG T -phosphorylation. Besides, *uPA* primers were as follows: forward primer; CTGTGACTGTC TAAATGGAGG; and the reverse primer; GACGATGTAGTCCT CCTTCTT (Nielsen *et al*, 2004).

Preliminary trials were undertaken to assure that results were accurate and reliable. We utilised highly specific hybridisation probes and primers to maintain high specificity for target genes and thereby reduce false positive outcomes.

RT–PCR conditions

PCR amplification was performed using a quantitative fluorescence LightCycler™ (Roche Diagnostics, Mannheim, Germany) in a 20 μl reaction mixture containing 2 μl of LightCyclert FastStart DNA Master Hybridisation Probes (Roche, Diagnostics, Tokyo, Japan), 4.0 μl $MgCl_2$, 0.3 μM sense and antisense primers, 0.2 μM fluorescent probe, 0.2 μM LC-Red probe and 5 μl of undiluted template cDNA in LightCyclert capillaries (Roche Diagnostics, Tokyo, Japan). The amplification of *CEA* profile consisted of one cycle at 95°C for 10 min (denaturation) followed by 45 cycles of 95°C for 15 s, 56°C for 15 s and 72°C for 13 s. The amplification of *CK-7* profile consisted of one cycle at 95°C for 10 min (denaturation) followed by 50 cycles of 95°C for 10 s, 60°C for 12 s and 72°C for 10 s. The amplification of *CK-19* profile consisted of one cycle at 95°C for 10 min (denaturation) followed by 45 cycles of 95°C for 10 s, 60°C for 15 s and 72°C for 16 s. The amplification of *uPAR* profile consisted of one cycle at 95°C for 10 min (denaturation) followed by 40 cycles of 95°C for 10 s, 62°C for 15 s and 72°C for 8 s. The amplification of *GAPDH* profile consisted of one cycle at 95°C for 10 min (denaturation) followed by 40 cycles of 95°C for 15 s, 60°C for 15 s and 72°C for 13 s. The amplification of uPA was as follows: 5 min at 94°C, 27 cycles of 1 min at 94°C, 1 min at 56°C, 1 min at 72°C, then 10 min at 72°C (Nielsen *et al*, 2004). Real-time PCR was monitored by measuring fluorescent signals at the end of the annealing phase for each cycle. All primers and probes were synthesized and purified by reverse phase high-performance liquid chromatography and the optimal reagent concentrations and PCR cycling conditions were established and each run of RT–PCR included positive controls synthesized from plasmids by the Nippon Gene Research Laboratories (Sendai, Japan). Real-time RT–PCR assays were repeated in triplicate and adapted the mean value. Quantification data were analysed using the Light-Cycler™ software (Roche Diagnostics, Tokyo, Japan).

Data analysis

A standard curve was prepared with 200–20 000 copies of purified plasmids containing *CEA*, *CK-7*, *CK-19*, *uPAR* and *GAPDH*. After proportional baseline adjustment, the fit point method was employed to determine the cycle in which the log-linear signal was first distinguishable from the baseline, and then that cycle number was used as a crossing-point value (Marutsuka *et al*, 2003). The standard curve was produced by measuring the crossing point of each standard value and plotting them against the logarithmic value of concentrations. Those concentrations were calculated by plotting their crossing points against the standard curve.

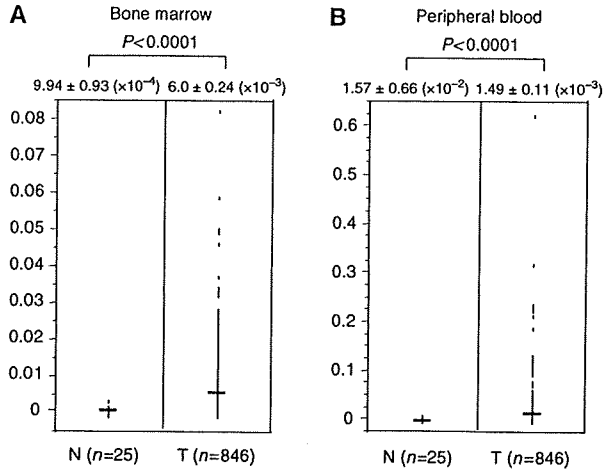

Figure 1 Comparison of *uPAR* mRNA expression between control gastric cancer patients in bone marrow (**A**) and peripheral blood (**B**). Horizontal lines indicate the mean expression levels in control and gastric cancer patients. In bone marrow and peripheral blood, the value of the *uPAR* expression of gastric cancer patients was significantly higher ($P<0.0001$) than those of control cases. The *P*-value was calculated by a student's *t*-test.

Expression of CEA, CK-7, CK-19 and *uPAR* was adjusted in each case for GAPDH expression. We set cutoff values for those expression ratios (*CEA/GAPDH, CK-7/GAPDH, CK-19/GAPDH, uPAR/GAPDH*) as the highest value for each marker in 25 normal controls. We distributed high level as 'positive' and low level as 'negative' than the cutoff value. For continuous variables, the data were expressed as the mean ± s.d. Statistical analysis of group differences was performed using the χ^2 test and the Student's *t*-test. Logistic regression model was used to identify the independent predictors of distant metastasis. All tests were analysed using JMP software (SAS Institute Inc., Cary, NC, USA). Statistical significance was determined as *P*-value from two-sided tests of less than 0.05.

RESULTS

Expression of *uPAR* mRNA in BM and PB of gastric cancer patients

In BM, the value of the *uPAR* expression of gastric cancer patients (6.0 ± 0.24 ($\times 10^{-3}$)) was significantly higher ($P<0.0001$) than those of control cases (9.94 ± 0.93 ($\times 10^{-4}$)), as shown in Figure 1. In PB, the value of the *uPAR* expression of gastric cancer patients (1.49 ± 0.11 ($\times 10^{-2}$)) was also significantly higher ($P<0.0001$) than those of control cases (1.57 ± 0.66 ($\times 10^{-3}$)).

Clinical magnitude of *uPAR* expression in gastric cancer patients

The correlations between the results for the *uPAR* mRNA level and clinicopathologic factors are summarised in Table 1. Using each cutoff value, 431 (50.9%) and 404 (47.8%) of 846 patients were estimated to be positive for *uPAR* mRNA in BM and PB, respectively.

In BM, the significantly higher population of the *uPAR* mRNA-positive cases belongs to the following clinical subgroups: invasion deeper than the muscularis propria ($P=0.015$), perioperative overt metastases (including liver and/or lung and/or distant lymph node metastasis, $P=0.044$) and postoperative recurrence ($P=0.010$).

In PB, the higher expression was observed significantly in subgroup invasion deeper than the muscularis propria ($P=0.009$), perioperative overt metastases ($P=0.002$), venous invasion ($P=0.039$), and the clinical stage ($P=0.008$).

Multivariate analysis for distant metastasis

Univariate and multivariate logistic regression analyses were performed on cases with distant metastasis (Table 2). Univariate regression analysis showed that the following factors were significantly associated with distant metastasis: histological grade, tumour size, lymph node metastasis, lymphatic invasion, venous invasion and *uPAR* mRNA expressions in BM and PB ($P<0.05$), respectively. Multivariate regression analysis indicated that *uPAR* mRNA high expression group in PB (relative risk (RR); 1.85, 95 % confidence interval (CI); 1.08–3.23, $P=0.03$) was an independent predictor for distant metastasis next to the incidence lymph node metastasis (RR; 6.50, 95 % CI; 2.99–15.77, $P<0.0001$) and depth of tumour invasion (RR; 28.2, 95% CI; 14.3–70.0, $P<0.0001$).

The comparison of *uPA* and *uPAR* expression in representative gastric cancer cases

The potential importance of uPAR for the development of minimal residual disease in solid cancer has been focused on for recent two decades; however, several studies revealed that the relevance of a ligand for *uPAR*, *uPA* in mediating tumour-associated proteolysis, invasion and metastasis together with *uPAR* expression (Andreasen *et al*, 2000). We examined *uPA* expression in bone marrow and peripheral blood in representative 83 cases of gastric cancer, including 18 cases of liver and/or lung metastasis, and 12 cases of recurrence of disease among 846 cases of gastric cancer. As we showed in Table 3, we found that *uPA* expression in bone marrow from gastric cancer is correlated with the incidence of lymph node metastasis and recurrence of gastric cancer cases as *uPAR* expression.

The clinical significance of both positive ITCs and positive *uPAR* expression

We identified 66 cases out of 846 (7.8%) that were positive for expression of CEA in bone marrow, whereas 108 (12.7%) were positive in peripheral blood. As for CK-7, 71 patients (8.4%) and 147 cases (20.6%) were positive in bone marrow and in peripheral blood, respectively. Cytokeratin-19 expression was detected in bone marrow in 153 cases (18.1%) and in 251 cases (29.7%) in peripheral blood. Gastric cancer cases with positive expression of any one of the three markers were defined as ITC-positive in bone marrow or peripheral blood. As outlined above, ITCs were detected in 260 (30.7%) cases in bone marrow and 417 (49.3%) cases in peripheral blood.

Moreover, we extracted 126 cases (14.9%) in BM and 200 cases (23.6%) in PB of positive ITCs and positive *uPAR* expression cases. Table 4 shows the clinicopathologic data and positive ITCs and positive uPAR cases from the 846 gastric cancer patients. In BM, the incidence of lymph node metastasis was significantly higher ($P=0.012$) in the both positive group (65 of 126, 51.6%) than in the other group (285 of 720, 39.6%), and the incidence of lymphatic invasion was significantly higher ($P=0.009$) in the both positive group (67 of 126, 53.2%) than in the other group (293 of 720, 40.7%). Moreover, the clinical stage was significantly higher ($P=0.024$) in the both positive group (42 of 126, 33.3%) than in the other group (170 of 720, 23.4%). In PB, there was no significance between the both positive group and the other group.

DISCUSSION

In this study, we examined the clinicopathologic significance of *uPAR* expression in BM and PB in 846 cases of gastric cancer, and found that the depth of tumour invasiveness in the primary

Table 1 Relationship between uPAR expression in bone marrow and peripheral blood and clinicopathologic findings

		uPAR expression in bone marrow			uPAR expression in peripheral blood		
Total	**846**	**Positive $n=431$ (50.9%)**	**Negative $n=415$ (49.1%)**	***P*-value**	**Positive $n=404$ (47.8%)**	**Negative $n=442$ (52.2%)**	***P*-value**
Age (mean ± s.d.[a])		60.4 ± 0.55	62.7 ± 0.56	NS	61.5 ± 0.57	61.6 ± 0.55	NS
Gender				0.233			0.688
Male	567	297 (69.1)	270 (65.2)		268 (66.5)	299 (67.8)	
Female	279	134 (30.9)	145 (34.8)		136 (33.5)	143 (32.2)	
Histology				0.127			0.174
Differentiated	188	105 (24.4)	83 (20.0)		98 (24.3)	90 (20.4)	
Undifferentiated	658	326 (75.6)	332 (80.0)		306 (75.7)	352 (79.6)	
pT				0.015			0.009
pT1/T2	657	320 (74.3)	337 (81.2)		298 (73.8)	359 (81.2)	
pT3/T4	189	111 (25.7)	78 (18.8)		106 (26.2)	83 (18.8)	
pN				0.707			0.072
pN0	496	250 (58.0)	246 (59.3)		224 (55.5)	272 (61.5)	
pN1	350	181 (42.0)	169 (40.7)		180 (44.5)	170 (38.5)	
pM (Distant metastasis[a])				0.044			0.002
pM0	743	369 (85.6)	374 (90.1)		340 (84.2)	403 (91.2)	
pM1	103	62 (14.4)	41 (9.9)		64 (15.8)	39 (8.8)	
Postoperative recurrence				0.01			0.115
Non recurrence	833	420 (97.5)	413 (99.5)		395 (97.8)	438 (99.1)	
Recurrence	13	11 (2.5)	2 (0.5)		9 (2.2)	4 (0.9)	
Lymphatic invasion				0.617			0.16
Negative	486	244 (58.3)	242 (58.3)		222 (55.0)	264 (59.7)	
Positive	360	187 (56.6)	173 (41.7)		182 (45.0)	178 (40.3)	
Venous invasion				0.425			0.039
Negative	702	362 (83.9)	340 (81.9)		324 (80.2)	378 (85.5)	
Positive	144	69 (16.1)	75 (18.1)		80 (19.8)	64 (14.5)	
Stage				0.081			0.008
I, II	634	312 (72.4)	322 (77.6)		286 (70.8)	348 (78.7)	
III, IV	212	119 (27.6)	93 (22.4)		118 (29.2)	94 (21.3)	

[a]Gastric cancer case with liver (H1) and/or lung metastasis (M1), cytology positive of peritoneal washes (CY1), peritoneal dissemination (P), and lymph node metastasis in the distant region (N3).

Table 2 Univariate and multivariate analysis for distant metastasis (logistic regression model)

	Univariate analysis			Multivariate analysis		
	RR	**95% CI**	***P*-value**	**RR**	**96% CI**	***P*-value**
Histological grade (Differentiated/undifferentiated)	2.35	1.31–2.35	<0.0001	0.58	0.24–1.45	0.239
pT (Depth of tumour invasion)	49.91	27.36–99.07	<0.0001	28.17	14.30–60.95	<0.0001
pN (Lymph node metastasis)	22.78	11.56–51.49	<0.0001	6.5	2.99–15.77	<0.0001
Lymphatic invasion	12.12	6.89–23.12	<0.0001	—	—	—
Venous invasion	4.55	2.91–7.10	<0.0001	1.61	0.90–2.88	0.106
uPAR mRNA expression in bone marrow	1.53	1.01–2.35	0.046	—	—	—
uPAR mRNA expression in peripheral blood	1.95	1.28–2.99	0.002	1.85	1.08–3.23	0.0207

tumour was significantly higher in cases of *uPAR* (+) in BM and/or PB than *uPAR*(−) cases. In addition, we disclosed an evidence of the concordant relationship between the venous permeation in primary cancer and the incidence of *uPAR* expression. In spite of the strong association between tumour invasiveness, the presence of *uPAR* in PB was uncovered to be much more intimate to the incidence of metastasis and could be an independent prognostic indicator for hematogenous metastasis. Therefore, we consider that *uPAR* might play a consecutive role in cancer cells to invade into vessels and/or invading into the metastatic site. Furthermore, the clinical relevance of *uPAR* in bone marrow was observed with the incidence of recurrence, not with the synchronous distant metastasis. There was a possible explanation which is as follows, Kook *et al* (1994) reported that *uPAR* can play a role in tumour cell dormancy. They reported that a *uPAR*-antisense strategy in a human squamous carcinoma cell line resulting in a significant reduction of *uPAR* gene expression, induced tumour cell dormancy in their study. Besides, Laufs *et al* (2006) described this point in the review concerning *uPAR*. Therefore, the abundant expression of *uPAR* in bone marrow might indicate the presence of many dormant cells giving rise to recurrence in the future.

In an earlier study by Jauch *et al* (1996) uPAR is a glycosylphosphatidylinositol-anchored glycoprotein localised on the outer layer of the plasma membrane of cells, and it binds to its specific ligands such as urokinase-type plasminogen activator (uPA). In this study, we confirmed the concordant relationship between *uPAR* and *uPA* in bone marrow and peripheral blood indicating that both proteins have a synergistic role with each other in lymph node metastasis and recurrence of gastric cancer. However, uPAR activation ultimately leads to degradation of the extracellular matrix and fascinates cellular movement for tumour cells, which appears to be necessary for diverse

Table 3 Clinicopathologic significance of uPAR and uPA expressions in bone marrow (BM) and peripheral blood (PB) from gastric cancer cases

		uPAR-BM			uPAR-PB			uPA-BM			uPA-PB		
	n	Mean	s.d.	*P*-value	Mean	s.d.	*P*-value	Mean	s.d.	*P*-value	Mean	s.d.	*P*-value
ly				NS			NS			NS			NS
−	58	8.9E-03	6.2E-03		1.4E-02	8.1E-03		2.1E-02	1.3E-02		2.4E-03	2.2E-03	
+	25	1.1E-02	1.1E-02		1.3E-02	9.5E-03		2.2E-02	1.8E-02		3.1E-03	7.3E-03	
v				NS			NS			NS			NS
−	65	9.7E-03	7.8E-03		1.3E-02	8.3E-03		2.1E-02	1.2E-02		2.2E-03	2.1E-03	
+	18	9.3E-03	9.0E-03		1.5E-02	9.2E-03		2.4E-02	2.0E-02		4.0E-03	8.6E-03	
n				**0.0006**			NS			**0.0002**			NS
−	62	7.9E-03	5.4E-03		1.3E-02	8.5E-03		1.8E-02	1.2E-02		2.8E-03	5.1E-03	
+	21	1.5E-02	1.2E-02		1.3E-02	8.7E-03		3.1E-02	1.7E-02		2.1E-03	1.3E-03	
cy				NS			NS			NS			NS
−	71	9.2E-03	7.9E-03		1.3E-02	8.4E-03		2.1E-02	1.5E-02		2.5E-03	4.6E-03	
+	16	1.3E-02	8.5E-03		1.5E-02	8.1E-03		2.6E-02	1.5E-02		3.2E-03	2.6E-03	
P				NS			NS			NS			NS
−	80	9.5E-03	7.9E-03		1.3E-02	8.4E-03		2.1E-02	1.5E-02		2.6E-03	4.5E-03	
+	8	1.3E-02	9.4E-03		1.4E-02	7.6E-03		2.6E-02	1.6E-02		2.7E-03	1.9E-03	
met				NS			NS			NS			**0.0265**
−	70	9.2E-03	7.9E-03		1.3E-02	8.2E-03		2.0E-02	1.3E-02		2.1E-03	1.9E-03	
+	18	1.2E-02	8.7E-03		1.6E-02	8.4E-03		2.8E-02	1.9E-02		4.6E-03	8.7E-03	
rec				**0.0072**			NS			**0.0409**			NS
−	76	8.9E-03	6.6E-03		1.4E-02	8.6E-03		2.0E-02	1.5E-02		2.6E-03	4.6E-03	
+	12	1.6E-02	1.3E-02		1.1E-02	5.9E-03		3.0E-02	1.3E-02		2.2E-03	1.5E-03	

cy = cytology of peritoneal washes; ly = lymphatic permiation; met = liver and/or lung metastasis; n = lymph node metastasis; p = peritoneal dissemination; rec = recurrence; s.d. = standard deviation; v = vascular permiation. Significant differences ($P<0.05$) were described in bold letters.

functions including local invasion and metastasis of tumour cells (Heiss *et al*, 1997).

Then, the second point is what is the origin of cells expressing *uPAR* gene in BM and especially in PB. As a matter of fact, Heiss *et al* (1995, 1997, 2002) reported that the gastric cancer patients with cells with uPAR protein expression by immunocytology showed significantly poorer prognosis than cases without uPAR expression by Kaplan–Meier analysis in the previous study (Jauch *et al*, 1996; Hardingham *et al*, 2000). They confirmed that uPAR protein expressing cells on the surface cells was a cancer cell by immunocytological study. Their study strongly supported the current study by quantitative RT–PCR assay that the detected *uPAR* expression by RT–PCR should be originally from gastric cancer cells, and gastric cancer patients with cancer cells with the invasive ability especially in PB. Moreover, we additionally disclosed that cancer patients with simultaneous expression uPAR and epithelial cell markers, *CEA*, *CK19* and *CK7* showed a relatively poorer prognosis than ITCs alone. Gastric cancer cell isolated from primary cancer is circulating in the peripheral blood and bone marrow ubiquitously among whole stages (Mimori *et al*, 2008); however, isolated cancer cells with several potential abilities must be required to form metastasis. According to this study, we concluded that *uPAR*-expressing isolated tumour cells are important in the determination of recurrence through lymph node metastasis.

On the contrary to the hypothesis of the origin of uPAR expression in cancer cells, several studies have uncovered findings of the uPAR from host side cells in BM or PB from cancer patients. Pyke *et al* (1993) reported the abundant expression of uPAR in macrophage (Dubuisson *et al*, 2000), and Sugai *et al* (2004) disclosed that advances in gastric cancer cases indicated the activation of inflammatory cytokines, such as IL-10 and IL-12 from macrophages. Furthermore, Hildenbrand *et al* (1998) mentioned that the abundant expression of uPAR was observed in endothelial cells, which has been recently really focused on as the key player for the initial development of metastasis. Mancuso *et al* (2001) reported that the number of circulating endothelial cells (CECs) in PB from cancer patients are more than that in healthy volunteers (Beerepoot *et al*, 2004). Asahara *et al* (1997) reported that bone marrow-derived endothelial cell progenitor cells were disseminated to the neovascularisation of the cellular surface of malignant cells (Peters *et al*, 2005). In addition, EPC-specific gene, Id-1, was reported to be identified and its consecutive role for metastasis has been reported in the recent study. Therefore, we considered that the presence of CEC or EPC in PB should be important to form metastasis, and our current study elucidated the role of uPAR especially in PB as the independent marker for metastasis.

In this study, we concluded that the RT–PCR assay for *uPAR* expression in PB can be one of the favourite tumour markers to predict DFS in gastric cancer outpatients. Then, we disclosed the abundant expression of uPAR in gastric cancer cases with invasion and with venous invasion abilities. Earlier Heiss *et al* distinctively disclosed that uPAR expression in BM and PB in gastric cancer is originally from cancer cells themselves (Heiss *et al*, 1995). However, as the clinicopathologic significance and the predictive role for metastasis is much more consecutive in uPAR in PB than in BM, uPAR might be originally expressed in endothelial (progenitor) cells as the host side reaction in gastric cancer patients. Further study will be required to address this controversial issue.

ACKNOWLEDGEMENTS

This work was supported by the following grant sponsors: CREST, Japan Science and Technology Agency (JST); Japan Society for the

Table 4 Relationship between epithelial marker and uPAR expression in bone marrow and peripheral blood and clinicopathologic findings

		Epithelial marker and uPAR expression in BM			Epithelial marker and uPAR expression in PB		
	Total (n = 846)	Both positive n = 126	Others n = 720	P-value	Both positive n = 200	Others n = 646	P-value
Age (mean ± s.d.*)		60.9 ± 0.97	61.6 ± 0.43	NS	60.8 ± 0.81	61.7 ± 0.45	NS
Gender				0.403			
Male	567	88 (69.8)	479 (66.5)		130 (65.0)	437 (67.6)	0.526
Female	279	38 (30.2)	241 (33.5)		70 (35.0)	209 (32.4)	
Histology				0.645			
Differentiated	188	30 (23.8)	158 (21.9)		45 (22.5)	143 (22.1)	0.914
Undifferentiated	658	96 (76.2)	562 (78.1)		155 (77.5)	503 (77.9)	
pT				0.183			
pT1/T2	657	92 (73.0)	565 (78.5)		147 (73.5)	510 (79.0)	0.11
pT3/T4	189	34 (27.0)	155 (21.5)		53 (26.5)	136 (21.0)	
pN					0.012		
pN0	496	61 (48.4)	435 (60.4)		112 (56.0)	384 (59.4)	0.389
pN1	350	65 (51.6)	285 (39.6)		88 (44.0)	262 (40.6)	
pM (Distant metastasis)				0.108			
pM0	743	105 (83.3)	638 (88.6)		170 (85.0)	573 (88.7)	0.171
pM1	103	21 (16.7)	82 (11.4)		30 (15.0)	73 (11.3)	
Postoperative recurrence				0.145			
Non recurrence	833	122 (96.8)	711 (98.8)		197 (98.5)	636 (98.5)	0.961
Recurrence	13	4 (3.2)	9 (1.2)		3 (1.5)	10 (1.5)	
Lymphatic invasion				0.009			
Negative	486	59 (46.8)	427 (59.3)		117 (58.5)	369 (57.1)	0.73
Positive	360	67 (53.2)	293 (40.7)		83 (41.5)	277 (42.9)	
Venous invasion				0.102			
Negative	702	98 (77.8)	604 (83.9)		162 (81.0)	540 (83.6)	0.399
Positive	144	28 (22.2)	116 (16.1)		38 (19.0)	106 (16.4)	
Stage				0.024			
I, II	634	84 (66.7)	550 (76.4)		141 (70.5)	493 (76.3)	0.101
III, IV	212	42 (33.3)	170 (23.4)		59 (29.5)	153 (23.7)	

*s.d. = standard deviation.

Promotion of Science (JSPS) Grant-in-Aid for Scientific Research, Grant numbers 17109013, 17591411, 17591413, 18390367, 18590333, 18659384 and 18790964; The Ministry of Education, Culture, Sports, Science and Technology (MEXT) Grant-in-Aid for Scientific Research on Priority Areas, Grant number 18015039; Third Term Comprehensive 10-year Strategy for Cancer Control, Grant number 16271201.

REFERENCES

Allgayer H, Heiss MM, Riesenberg R, Grutzner KU, Tarabichi A, Babic R, Schildberg FW (1997) Urokinase plasminogen activator receptor (uPA-R): one potential characteristic of metastatic phenotypes in minimal residual tumor disease. *Cancer Res* **57**: 1394–1399

Andreasen PA, Egelund R, Petersen HH (2000) The plasminogen activation system in tumor growth, invasion, and metastasis. *Cell Mol Life Sci* **57**: 25–40

Asahara T, Murohara T, Sullivan A, Silver M, van der Zee R, Li T, Witzenbichler B, Schatteman G, Isner JM (1997) Isolation of putative progenitor endothelial cells for angiogenesis. *Science* **275**: 964–967

Beerepoot LV, Mehra N, Vermaat JS, Zonnenberg BA, Gebbink MF, Voest EE (2004) Increased levels of viable circulating endothelial cells are an indicator of progressive disease in cancer patients. *Ann Oncol* **15**: 139–145

Bessa X, Pinol V, Castellvi-Bel S, Piazuelo E, Lacy AM, Elizalde JI, Pique JM, Castells A (2003) Prognostic value of postoperative detection of blood circulating tumor cells in patients with colorectal cancer operated on for cure. *Ann Surg* **237**: 368–375

Dubuisson L, Monvoisin A, Nielsen BS, Le Bail B, Bioulac-Sage P, Rosenbaum J (2000) Expression and cellular localisation of the urokinase-type plasminogen activator and its receptor in human hepatocellular carcinoma. *J Pathol* **190**: 190–195

Hardingham JE, Hewett PJ, Sage RE, Finch JL, Nuttall JD, Kotasek D, Dobrovic A (2000) Molecular detection of blood-borne epithelial cells in colorectal cancer patients and in patients with benign bowel disease. *Int J Cancer* **89**: 8–13

Heiss MM, Allgayer H, Gruetzner KU, Babic R, Jauch KW, Schildberg FW (1997) Clinical value of extended biologic staging by bone marrow micrometastases and tumor-associated proteases in gastric cancer. *Ann Surg* **226**: 736–744; discussion 744–5

Heiss MM, Allgayer H, Gruetzner KU, Funke I, Babic R, Jauch KW, Schildberg FW (1995) Individual development and uPA-receptor expression of disseminated tumour cells in bone marrow: a reference to early systemic disease in solid cancer. *Nat Med* **1**: 1035–1039

Heiss MM, Simon EH, Beyer BC, Gruetzner KU, Tarabichi A, Babic R, Schildberg FW, Allgayer H (2002) Minimal residual disease in gastric cancer: evidence of an independent prognostic relevance of urokinase receptor expression by disseminated tumor cells in the bone marrow. *J Clin Oncol* **20**: 2005–2016

Hellman S (1997) Stopping metastases at their source. *N Engl J Med* 337: 996–997

Hildenbrand R, Glienke W, Magdolen V, Graeff H, Stutte HJ, Schmitt M (1998) Urokinase receptor localization in breast cancer and benign lesions assessed by *in situ* hybridization and immunohistochemistry. *Histochem Cell Biol* 110: 27–32

Iinuma H, Okinaga K, Egami H, Mimori K, Hayashi N, Nishida K, Adachi M, Mori M, Sasako M (2006) Usefulness and clinical significance of quantitative real-time RT-PCR to detect isolated tumor cells in the peripheral blood and tumor drainage blood of patients with colorectal cancer. *Int J Oncol* 28: 297–306

Ikeguchi M, Kaibara N (2005) Detection of circulating cancer cells after a gastrectomy for gastric cancer. *Surg Today* 35: 436–441

Jauch KW, Heiss MM, Gruetzner U, Funke I, Pantel K, Babic R, Eissner HJ, Riethmueller G, Schildberg FW (1996) Prognostic significance of bone marrow micrometastases in patients with gastric cancer. *J Clin Oncol* 14: 1810–1817

Kook YH, Adamski J, Zelent A, Ossowski L (1994) The effect of antisense inhibition of urokinase receptor in human squamous cell carcinoma on malignancy. *EMBO J* 13: 3983–3991

Laufs S, Schumacher J, Allgayer H (2006) Urokinase-receptor (u-PAR): an essential player in multiple games of cancer: a review on its role in tumor progression, invasion, metastasis, proliferation/dormancy, clinical outcome and minimal residual disease. *Cell Cycle* 5: 1760–1771

Lecomte T, Berger A, Zinzindohoue F, Micard S, Landi B, Blons H, Beaune P, Cugnenc PH, Laurent-Puig P (2002) Detection of free-circulating tumor-associated DNA in plasma of colorectal cancer patients and its association with prognosis. *Int J Cancer* 100: 542–548

Mancuso P, Burlini A, Pruneri G, Goldhirsch A, Martinelli G, Bertolini F (2001) Resting and activated endothelial cells are increased in the peripheral blood of cancer patients. *Blood* 97: 3658–3661

Marutsuka T, Shimada S, Shiomori K, Hayashi N, Yagi Y, Yamane T, Ogawa M (2003) Mechanisms of peritoneal metastasis after operation for non-serosa-invasive gastric carcinoma: an ultrarapid detection system for intraperitoneal free cancer cells and a prophylactic strategy for peritoneal metastasis. *Clin Cancer Res* 9: 678–685

Masuda TA, Inoue H, Sonoda H, Mine S, Yoshikawa Y, Nakayama K, Nakayama K, Mori M (2002) Clinical and biological significance of S-phase kinase-associated protein 2 (Skp2) gene expression in gastric carcinoma: modulation of malignant phenotype by Skp2 overexpression, possibly via p27 proteolysis. *Cancer Res* 62: 3819–3825

Masuda TA, Kataoka A, Ohno S, Murakami S, Mimori K, Utsunomiya T, Inoue H, Tsutsui S, Kinoshita J, Masuda N, Moriyama N, Mori M (2005) Detection of occult cancer cells in peripheral blood and bone marrow by quantitative RT-PCR assay for cytokeratin-7 in breast cancer patients. *Int J Oncol* 26: 721–730

Mimori K, Fukagawa T, Kosaka Y, Kita Y, Ishikawa K, Etoh T, Iinuma H, Sasako M, Mori M (2008) Hematogenous metastasis in gastric cancer requires isolated tumor cells and expression of vascular endothelial growth factor receptor-1. *Clin Cancer Res* 14: 2609–2616

Mori M, Mimori K, Inoue H, Barnard GF, Tsuji K, Nanbara S, Ueo H, Akiyoshi T (1995) Detection of cancer micrometastases in lymph nodes by reverse transcriptase-polymerase chain reaction. *Cancer Res* 55: 3417–3420

Mori M, Mimori K, Ueo H, Karimine N, Barnard GF, Sugimachi K, Akiyoshi T (1996) Molecular detection of circulating solid carcinoma cells in the peripheral blood: the concept of early systemic disease. *Int J Cancer* 68: 739–743

Mori M, Mimori K, Ueo H, Tsuji K, Shiraishi T, Barnard GF, Sugimachi K, Akiyoshi T (1998) Clinical significance of molecular detection of carcinoma cells in lymph nodes and peripheral blood by reverse transcription-polymerase chain reaction in patients with gastrointestinal or breast carcinomas. *J Clin Oncol* 16: 128–132

Natsugoe S, Nakashima S, Nakajo A, Matsumoto M, Okumura H, Tokuda K, Miyazono F, Kijima F, Aridome K, Ishigami S, Takao S, Aikou T (2003) Bone marrow micrometastasis detected by RT-PCR in esophageal squamous cell carcinoma. *Oncol Rep* 10: 1879–1883

Nielsen TO, Andrews HN, Cheang M, Kucab JE, Hsu FD, Ragaz J, Gilks CB, Makretsov N, Bajdik CD, Brookes C, Neckers LM, Evdokimova V, Huntsman DG, Dunn SE (2004) Expression of the insulin-like growth factor I receptor and urokinase plasminogen activator in breast cancer is associated with poor survival: potential for intervention with 17-allylamino geldanamycin. *Cancer Res* 64: 286–291

Peters BA, Diaz LA, Polyak K, Meszler L, Romans K, Guinan EC, Antin JH, Myerson D, Hamilton SR, Vogelstein B, Kinzler KW, Lengauer C (2005) Contribution of bone marrow-derived endothelial cells to human tumor vasculature. *Nat Med* 11: 261–262

Pyke C, Graem N, Ralfkiaer E, Ronne E, Hoyer-Hansen G, Brunner N, Dano K (1993) Receptor for urokinase is present in tumor-associated macrophages in ductal breast carcinoma. *Cancer Res* 53: 1911–1915

Sadahiro S, Suzuki T, Ishikawa K, Saguchi T, Maeda Y, Yasuda S, Makuuchi H, Yurimoto S, Murayama C (2005) Detection of carcinoembryonic antigen messenger RNA-expressing cells in portal and peripheral blood during surgery does not influence relapse in colorectal cancer. *Ann Surg Oncol* 12: 988–994

Sobin LH, Fleming ID (1997) TNM Classification of Malignant Tumors, fifth edition (1997). Union Internationale Contre le Cancer and the American Joint Committee on Cancer. *Cancer* 80: 1803–1804

Sugai H, Kono K, Takahashi A, Ichihara F, Kawaida H, Fujii H, Matsumoto Y (2004) Characteristic alteration of monocytes with increased intracellular IL-10 and IL-12 in patients with advanced-stage gastric cancer. *J Surg Res* 116: 277–287

Yamaguchi K, Takagi Y, Aoki S, Futamura M, Saji S (2000) Significant detection of circulating cancer cells in the blood by reverse transcriptase-polymerase chain reaction during colorectal cancer resection. *Ann Surg* 232: 58–65

Enhanced expression of *p210BCR/ABL* and aberrant expression of *Zfp423/ZNF423* induce blast crisis of chronic myelogenous leukemia

Kazuko Miyazaki,[1] Norimasa Yamasaki,[1] Hideaki Oda,[2] Takeshi Kuwata,[3] Yohei Kanno,[4] Masaki Miyazaki,[5] Yukiko Komeno,[6] Jiro Kitaura,[6] Zen-ichiro Honda,[7] Søren Warming,[8] Nancy A. Jenkins,[9] Neal G. Copeland,[9] Toshio Kitamura,[6] Takuro Nakamura,[4] and Hiroaki Honda[1]

[1]Department of Developmental Biology, Research Institute of Radiation Biology and Medicine, Hiroshima University, Hiroshima, Japan; [2]Department of Pathology, Tokyo Women's Medical University, Tokyo, Japan; [3]Pathology Section, Clinical Laboratory Division, National Cancer Center Hospital East, Chiba, Japan; [4]Division of Carcinogenesis, The Cancer Institute of Japanese Foundation for Cancer Research, Tokyo, Japan; [5]Department of Immunology, Graduate School of Biomedical Sciences, Hiroshima University, Hiroshima, Japan; [6]Division of Cellular Therapy, The Institute of Medical Science, University of Tokyo, Tokyo, Japan; [7]Department of Allergy and Rheumatology, Graduate School of Medicine, University of Tokyo, Tokyo, Japan; [8]Department of Molecular Biology, Genentech, South San Francisco, CA; and [9]Cancer Genetics Laboratory, Institute of Molecular and Cell Biology, Singapore

Chronic myelogenous leukemia (CML) is a hematopoietic disorder originating from *p210BCR/ABL*-transformed stem cells, which begins as indolent chronic phase (CP) but progresses into fatal blast crisis (BC). To investigate molecular mechanism(s) underlying disease evolution, CML-exhibiting *p210BCR/ABL* transgenic mice were crossed with BXH2 mice that transmit a replication-competent retrovirus. Whereas nontransgenic mice in the BXH2 background exclusively developed acute myeloid leukemia, *p210BCR/ABL* transgenic littermates developed nonmyeloid leukemias, in which inverse polymerase chain reaction detected 2 common viral integration sites (CISs). Interestingly, one CIS was transgene's own promoter, which up-regulated *p210BCR/ABL* expression. The other was the 5′ noncoding region of a transcription factor, *Zfp423*, which induced aberrant *Zfp423* expression. The cooperative activities of *Zfp423* and *p210BCR/ABL* were demonstrated as follows: (1) introduction of *Zfp423* in *p210BCR/ABL* transgenic bone marrow (BM) cells increased colony-forming ability, (2) suppression of *ZNF423* (human homologue of *Zfp423*) in *ZNF423*-expressing, *p210BCR/ABL*-positive hematopoietic cells retarded cell growth, (3) mice that received a transplant of BM cells transduced with *Zfp423* and *p210BCR/ABL* developed acute leukemia, and (4) expression of *ZNF423* was found in human *BCR/ABL*-positive cell lines and CML BC samples. These results demonstrate that enhanced expression of *p210BCR/ABL* and deregulated expression of *Zfp423/ZNF423* contribute to CML BC. (Blood. 2009;113: 4702-4710)

Introduction

Chronic myelogenous leukemia (CML) is a hematopoietic disorder of multipotential stem cells, which exhibits excessive proliferation of immature and mature myeloid cells.[1,2] The cytogenetic hallmark of CML is the Ph chromosome, created by t(9;22)(q34;q11),[3] where the amino-terminal *BCR* gene on chromosome 22 is fused to most of the *ABL* proto-oncogene on chromosome 9, thereby creating an 8.5-kb *BCR/ABL* chimeric mRNA encoding a 210-kDa hybrid protein (p210BCR/ABL).[4-6] p210BCR/ABL possesses a much higher kinase activity in comparison with the normal 145-kDa c-ABL,[7] which is believed to play a critical role in the pathogenesis of the disease.

The clinical course of CML is characterized by hematologically and temporally distinct stages.[1,2] In the initial stage, called chronic phase (CP), the disease is indolent and the leukemic cells retain an ability to differentiate into mature granulocytes. After several years' duration of the chronic phase, however, the disease inevitably accelerates and ultimately progresses to the terminal fatal stage, called blast crisis (BC), which involves aggressive proliferation of immature blast cells. The frequent appearances of additional chromosomal abnormalities in the blast phase strongly suggest that superimposed genetic events would account for the disease evolution,[8] but the underlying molecular mechanism(s) has remained largely unknown.

To understand the complex processes involved in the clinical course of human CML, it is necessary to develop animal models that express *p210BCR/ABL* and recapitulate the clinical features of the disease. Major attempts have been focused on bone marrow transplantation (BMT) experiments. Mice that have been lethally irradiated and received a transplant of bone marrow (BM) cells infected with *p210BCR/ABL*-expressing retroviruses exhibited a CML-like myeloproliferative disorder.[9-11] On the other hand, generation of transgenic mice expressing *p210BCR/ABL* under various promoters also provides useful models.[12-17] We generated *p210BCR/ABL* transgenic mice using the promoter from the mouse *TEC* gene, a gene encoding protein-tyrosine kinase preferentially expressed in hematopoietic progenitor cells.[18,19] Although the founder mouse died of T-cell acute lymphoblastic leukemia (ALL) with a short latency, transgenic offspring reproducibly exhibited a myeloproliferative disorder after a long latency period.[14] Peripheral blood smear showed remarkable myeloid hyperplasia with maturation, the BM was hypercellular with a predominance of myeloid cells at various stages of differentiation, and the spleen was enlarged with proliferation and expansion of myeloid cells.[14] These

Submitted May 3, 2007; accepted January 29, 2009. Prepublished online as *Blood* First Edition paper, February 20, 2009; DOI 10.1182/blood-2007-05-088724.

The online version of this article contains a data supplement.

The publication costs of this article were defrayed in part by page charge payment. Therefore, and solely to indicate this fact, this article is hereby marked "advertisement" in accordance with 18 USC section 1734.

pictures represent cardinal features of human CML, allowing us to consider these transgenic mice an animal model for CML.

To examine whether this transgenic model is applicable for investigating pathogenic processes from CP to BC of CML, we crossed *p210BCR/ABL* transgenic mice with mice heterozygous for *p53*, a gene frequently inactivated in CML BC, and generated mice transgenic for *p210BCR/ABL* and heterozygous for *p53*.[20] Interestingly, *p210BCR/ABL* transgenic, *p53* heterozygous mice died of acute leukemia with a short latency, and the analysis of *p53* status revealed that the residual normal *p53* allele was frequently and preferentially lost in the tumor tissues.[20] In addition, we crossed *p210BCR/ABL* transgenic mice with *Dok-1/Dok-2* knockout mice and showed that the absence of Dok-1 and Dok-2 accelerated the disease phenotype and caused BC, defining the role of Dok-1 and Dok-2 in tumor suppression.[21] Based on these results, our transgenic mice can be regarded as a useful model for investigating molecular mechanism(s) underlying the progression from CP to BC of human CML.

In this report, to identify genes whose altered expression causes CML BC, *p210BCR/ABL* transgenic mice were subjected to retroviral insertional mutagenesis, by backcrossing to BXH2 mice, a recombinant inbred mouse strain that develop myeloid leukemia mainly due to a horizontally transmitted replication-competent retrovirus and intrinsic myeloid tropism induced by a mutation in the *Icsbp1/Irf8* locus.[22-24]

Methods

Mice

p210BCR/ABL transgenic mice were generated as described.[14] To allow for retroviral insertional mutagenesis, *p210BCR/ABL* transgenic males were backcrossed 4 generations to BXH2 females, because the ecotropic retrovirus in the BXH2 strain is transmitted to the progeny through the milk. Genotyping of the mice was carried out as described.[14] All the mice used in this study were kept according to the guidelines of the Institute of Laboratory Animal Science, Hiroshima University, and all murine studies were approved by the animal care committee at the Japanese Foundation for Cancer Research.

Hematologic and pathologic analyses

Peripheral blood counts were routinely examined. Smears and stamp specimens of leukemic tissues were stained with Wright-Giemsa (WG). Tissues from dead or moribund animals were fixed in 10% buffered formaldehyde and examined by light microscopy. All organs were examined grossly and representative slices were prepared for hematoxylin-eosin staining.

Southern and Northern blot analyses

To detect gene rearrangements, genomic DNAs were digested with appropriate restriction enzymes and blotted with a genomic fragment adjacent to the integration site. For transgene promoter, a *BglI-SmaI* fragment in the promoter region was used as a probe, and for *Zfp423*, a genomic fragment generated by polymerase chain reaction (PCR) (primer sequences are 5′-GTGCGCACGTTTGTGAGGAGCTATA-3′ and 5′-CCAGCTATTCTGTCCAGGAGCAAGA-3′), which corresponds to a part of the first intron, was used as a probe. To detect RNA expression, total RNA extracted using TRIzol (Invitrogen, Carlsbad, CA) or mRNA purified using Oligo-Tex (Takara Bio, Tokyo, Japan) was blotted with *p210BCR/ABL* cDNA, *Zfp423* cDNA, or a part of coding region of *ZNF423* cDNA generated by genomic PCR (primer sequences are 5′-CAACCAGAAACACAAGTGCCCCATG-3′ and 5′-GTTGCAGTGGAAGGCAGAGATGTTG-3′).

RT-PCR

RNA was extracted using TRI zol. Reverse-transcription (RT)–PCR was performed as described (primer sequences are 5′-GAATGTCATCGTCCACTCAGCC-3′ and 5′-GGCCACAAAATCATACAGTGCA-3′ for *p210BCR/ABL*, 5′-GAGGATACCCCTACGACGTG-3′ and 5′-GACTTGTCACGCTGTTCCTGTC-3′ for *Zfp423*, and 5′-GGCATCAACCACGAGTGTAAGC-3′ and 5′-CTTCTGCGGAGAGGTGTCCTGT-3′ for *ZNF423*).[25]

Western blot analysis

Proteins extraction and Western blot were performed as described.[14]

Flow cytometric analysis

Cells were stained with monoclonal antibodies and second reagents. FITC-, PE-, and biotin-labeled monoclonal antibodies were purchased from BD PharMingen (San Diego, CA; Thy-1.2, CD19, CD45R/B220, Mac-1, Gr-1, and CD3) or from eBioscience (San Diego, CA; CD43, IgM, BP-1, and CD20). Biotinylated antibodies were revealed with streptavidin-APC (BD PharMingen). Clone 2.4G2 anti-CD32:CD16 was used to block Fc receptors. Fluorescence-activated cell sorter (FACS) analysis was performed on a FACSCalibur flow cytometer (Becton Dickinson, Franklin Lakes, NJ), and the data were analyzed with FlowJo software (TreeStar, Ashland, OR).

Identification of retroviral integration sites

Genomic DNAs were digested with restriction enzymes, self-ligated, and subjected to inverse PCR as described,[22] except that the CUA and CAU repeats were deleted from the secondary PCR primers. The position mapping on the mouse chromosome was done by BLAST searching using the University of Colombo School of Computing (UCSC) Genome Bioinformatics database (http://genome.ucsc.edu/)[26] and the definition of a common integration site (CIS) was the same as in the mouse retrovirus tagged cancer gene database (RTCGD; http://rtcgd.abcc.ncifcrf.gov/).[23,27]

Retrovirus-mediated gene transfer, colony formation assay, and bone marrow transplantation

Retroviral preparation and retrovirus-mediated gene transfer were performed as described.[28] For colony assay, BM cells of 5-fluorouracil (5FU)–treated transgenic or nontransgenic littermates were cultured in αMEM plus 20% FCS supplemented with 10 ng/mL IL-6, 10 ng/mL IL-3, and 100 ng/mL SCF (R&D Systems, Minneapolis, MN). Retrovirus was generated using plat-E cells[29] and added into the medium containing BM cells with 6 mg/mL polybrene (Sigma-Aldrich, St Louis, MO), and retrovirus-infected BM cells were subjected to B-cell colony assay using MethoCult M3630 (StemCell Technologies, Vancouver, BC) that contains rhIL7. After 7 to 12 days' incubation, green colony numbers were counted under a fluorescent microscope.

For BM transplantation, BM cells extracted from 5FU-untreated Balb/c mice were cultured for 24 hours in IMDM plus 15% FCS supplemented with 10 ng/mL IL-6, 10 ng/mL IL-3, 100 ng/mL SCF, and 10 ng/mL IL-7 (R&D Systems). Retrovirus infection and BM transplantation were performed as described.[30]

Retrovirus-mediated transduction of shRNA for *ZNF423*

Two short hairpin RNA (shRNA) target sequences for *ZNF423* (5′-GACATACCAGTGCATCAAG-3′ for *shRNA*-1 and 5′-CTGTAAGTTCTGCAGCAAG-3′ for *shRNA*-2) were chosen according to the siRNA Hairpin Oligonucleotide Sequence Designer (Clontech, Mountain View, CA). Annealed double-strand oligonucleotides were subcloned into RNA-ready pSIREN-retroQ retroviral expression vector (Clontech). Human hematopoietic cells were first transduced with ecotropic retrovirus receptor (EcoRVR) to render these cells competent for ecotropic retrovirus infection.[31] Plat-E cells were then transfected with a pSIREN-retroQ vector harboring *shRNA* and the culture supernatant was used for infecting the ecotropic retrovirus to EcoRVR-expressing cells using Viro Mag (OZ Biosciences, Marseille, France). These procedures routinely yielded a high

infection efficiency (~ 60%) as judged by GFP fluorescence (not shown). Infected cells were selected with puromycin (0.4 mg/mL) for 2 weeks, subsequently cultured in puromycin-free medium for at least another 2 weeks, and subjected to Northern blot and cell proliferation assay.

Cell proliferation assay

On day 1, 10^5 cells of the parental and *shRNA*-transduced sublines were plated in a 10-cm^2 dish and cultured in RPMI plus 10% FCS. Cell numbers were counted on day 3 and day 5.

Cell lines and patient samples

Ph-positive and Ph-negative human hematopoietic cell lines were kindly provided by Drs Hiroya Aso (Hiroshima, Japan) and Toshiya Inaba (Hiroshima, Japan). Patient samples were taken after informed consent was obtained in accordance with the Declaration of Helsinki and approval from the institutional review board at Hiroshima University was granted.[32] Diagnosis of CML CP or CML BC (myeloid or B-lymphoid lineage) was performed based on morphologic, cytogenetic, immunophenotypic, and molecular analyses.

Results

Acute leukemias in *p210BCR/ABL* transgenic mice on a BXH2 background

To identify gene(s) whose alteration by retrovirus insertion contributes to blast crisis of CML, *p210BCR/ABL* transgenic mice were backcrossed to BXH2 mice that contain and transmit a replication-competent retrovirus. *p210BCR/ABL* transgenic and wild-type (nontransgenic) littermates from the N4 BXH2 backcross generation were used for this study (designated as p210BCR/ABL/BXH2 and WT/BXH2, respectively).

WT/BXH2 mice began to develop acute leukemia at 6 months after birth (Figure 1A thin continuous line). Macroscopically, the leukemic mice exhibited hepatosplenomegaly and lymph node (LN) swelling, which were occasionally associated with thymic enlargement. Pathologic analysis showed that leukemic cells having morphology of myeloblasts proliferated in the peripheral blood and infiltrated into the liver, spleen, LNs, and other tissues (data not shown). Flow cytometric analysis of the leukemic tissues showed that the blast cells were exclusively positive for Mac-1 and Gr-1 but negative for Thy1.2 and CD19, indicating that they all were of myeloid origin (data not shown).

In contrast to the WT/BXH2 mice, several p210BCR/ABL/BXH2 mice (named as nos. 30, 1, 17, 5, 18, and 23; Figure 1A thick continuous line) developed nonmyeloid leukemias with a shorter latency. Among them, 4 mice (nos. 30, 17, 18, and 23) displayed splenomegaly and LN swelling but did not show apparent hepatomegaly. The other 2 mice (nos. 1 and 5) exhibited massive thymic enlargement with pleural effusion and splenomegaly. Pathologic analysis showed that leukemic cells having morphology of lymphoblasts were evident in the peripheral blood and infiltration of the blast cells was observed in the LNs, liver, and other tissues examined (Figure 1B and not shown). Flow cytometric analysis revealed that the leukemic cells of the former 4 mice (nos. 30, 17, 18, and 23) were positive for CD19 but negative for Thy1.2, Mac-1, and Gr-1, and those of the latter 2 mice (nos. 1 and 5) were positive for Thy1.2 but negative for CD19, Mac-1, and Gr-1, indicating that they were of B-lymphoid and T-lymphoid origins, respectively (Figure 1C and not shown). Three $CD19^+$ samples (nos. 17, 18, and 30) were further analyzed with antibodies against CD20, B220, BP-1, CD43, and IgM to investigate the differentiation stages (pro-B, pre-B, or mature B). As shown in Figure S1 (available on the *Blood* website; see the Supplemental Materials link at the top of the online article), all the samples were positive for CD20, B220, BP-1, and CD43 but negative for IgM, indicating that they were pre–B-cell leukemias.

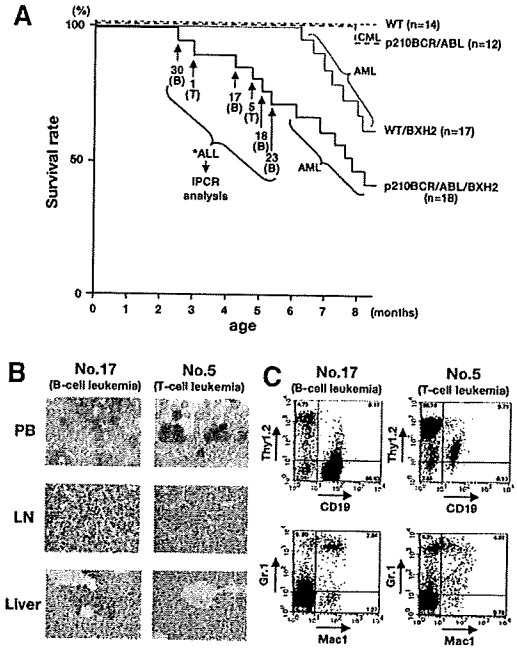

Figure 1. Survival curves and pathologic and flow cytometric analyses of leukemic mice. (A) Survival curves of the mice. The survival curves of WT/BXH2 and p210BCR/ABL/BXH2 are shown by thin and thick continuous lines, respectively, whereas those of BXH2-nonbackcrossed WT and p210BCR/ABL are shown by thin and thick dotted lines, respectively. As for the 6 p210BCR/ABL/BXH2 animals that died in a short latency and exhibited nonmyeloid phenotypes (nos. 30, 1, 17, 5, 18, and 23), the death points are indicated by → and the immunophenotypes of the disease are shown in the parentheses. T indicates T-cell leukemia; and B, B-cell leukemia. (B) Pathologic analysis of the leukemic mice. WG-stained peripheral blood smears (PB) and HE-stained lymph node (LN) and liver slices of a representative mouse for B-cell leukemia (no. 17) or T-cell leukemia (no. 5) are shown. PB smears show proliferation of blast cells and LN specimen shows the destruction of the basal structure by blast cell infiltration. In the liver, blast cells are observed around the vessel and in the sinusoids. (C) Flow cytometric analysis of mice that developed B-cell or T-cell leukemia. Blast cells of no. 17 were positive for CD19 but negative for Thy1.2, Mac-1, and Gr-1 and those of no. 5 were positive for Thy1.2 but negative for CD19, Mac-1, and Gr-1, indicating that they were of B- and T-lymphoid origins, respectively. The percentages of positive cells in each quadrant are shown.

The characteristics of the 6 p210BCR/ABL/BXH2 leukemic mice with an early disease onset are summarized in Table 1. As for the leukemias developed in the remaining p210BCR/ABL/BXH2 mice after 6 months of age, macroscopic appearances and the results of flow cytometric analysis were indistinguishable from those of the WT/BXH2 mice (data not shown). During the observation period, no mice developed hematologic disease in BXH2-nonbackcrossed WT mice and one mouse died of CML in BXH2-nonbackcrossed *p210BCR/ABL* transgenic mice (Figure 1A thin and thick dotted lines, respectively).

Enhanced expression of *p210BCR/ABL* and aberrant expression of *Zfp423* in the leukemic tissues with B-cell phenotype

We focused on the 6 p210BCR/ABL/BXH2 mice that developed nonmyeloid leukemias in a shortened period, because diseases in these mice would not be only due to the BXH2 background-derived intrinsic mechanism but caused by cooperation of *p210BCR/ABL*

Table 1. Characteristics of p210BCR/ABL/BHX2 mice with lymphoid leukemias

Mouse no.	Age at disease, mo	PB parameters			Macroscopic tumor sites	Surface markers	Diagnosis
		WBC, $\times 10^{9}$/L	Hb, g/L	Plt, $\times 10^{9}$/L			
30	2.6	11.2 (blast ~ 70%)	140	452	Spl, LN	Thy1.2$^-$, CD19$^+$, Gr.1$^-$, Mac1$^-$	B-cell leukemia
1	3.0	10.0 (blast ~ 60%)	124	238	Thy, Spl	Thy1.2$^+$, CD19$^-$, Gr.1$^-$, Mac1$^-$	T-cell leukemia
17	4.2	82.4 (blast ~ 100%)	109	525	Spl, LN	Thy1.2$^+$, CD19$^-$, Gr.1$^-$, Mac1$^-$	B-cell leukemia
5	4.8	22.0 (blast ~ 100%)	123	339	Thy, Spl, LN	Thy1.2$^-$, CD19$^+$, Gr.1$^-$, Mac1$^-$	T-cell leukemia
18	5.2	68.0 (blast ~ 100%)	118	345	Spl, LN	Thy1.2$^-$, CD19$^+$, Gr.1$^-$, Mac1$^-$	B-cell leukemia
23	5.4	19.8 (blast ~ 100%)	107	338	Spl, LN	Thy1.2$^-$, CD19$^+$, Gr.1$^-$, Mac1$^-$	B-cell leukemia

Spl indicates spleen; LN, lymph node; and Thy, thymus.

with retrovirus-inserted altered gene expression. To identify virus-affected genes in these mice, inverse PCR (iPCR) was performed and sequences of PCR fragments were subjected to BLAST searching using the UCSC Genome Bioinformatics database. Among candidate genes (listed in Table S1), we found 2 common integration sites (CISs) in B-lineage leukemias (shown by asterisks and in boldface in Table S1).

The first one was the promoter region of the mouse *TEC* gene. This CIS was found in nos. 17 and 30 and the viral integration sites were approximately 1.5-kb and approximately 200-bp upstream of the transcription initiation site,[19] respectively. Interestingly, in both cases, sequencing of the entire PCR fragment revealed that the mouse *TEC* promoter sequences were interrupted at +22 from the transcription initiation site and followed by human *BCR/ABL* cDNA. This result indicated that the integration sites were not in the endogenous mouse *TEC* gene but in the promoter region of the transgene itself. Another CIS observed in nos. 18 and 23 was in the noncoding region of the first exon of mouse *Zfp423* (*Zinc finger protein 423,* also known as *Early B-cell factor-associated zinc-finger protein, Ebfaz*) gene.[33] In these cases, the retroviruses were integrated almost in the same position, approximately 100-bp upstream of the translational initiation ATG.[33] The schematic models of the integration sites are shown in Figure 2A.

To confirm that these CISs were major integration sites in the leukemic samples, Southern blot was performed using a genomic DNA fragment adjacent to the integration site. DNA extracted from a spleen of a BXH2-nonbackcrossed *p210BCR/ABL* transgenic mouse was used as a negative control. As shown in Figure 2B, a rearranged band is evident in each sample (indicated by an arrowhead in Figure 2B), indicating that tumor cells with the CISs were predominant in the related tumors and were clonal in origin. The clonality and B-cell commitment of the leukemic cells in these mice (nos. 17, 30, 18, and 23) were further demonstrated by Southern blot using a mouse JH probe (Figure S2).

To investigate the alteration in gene expression of *p210BCR/ABL* and *Zfp423* by virus integration, RNAs extracted from tumor tissues of the 4 leukemic mice were blotted with *p210BCR/ABL* cDNA or mouse *Zfp423* cDNA. RNA extracted from a spleen of a BXH2-nonbackcrossed *p210BCR/ABL* transgenic mouse was used as control. The results are shown in upper panels of Figure 2C.

As for *p210BCR/ABL,* it is not surprising that the *p210BCR/ABL* message was not detected in the control transgenic mouse spleen (Figure 2C top left panel, "C"), because our previous data showed that the basal transgene expression was quite low, probably due to the nature of the promoter used (Honda et al[14] and data not shown). In contrast, a clear *p210BCR/ABL* message was evident in the tumors of nos. 17 and 30 (~ 7 kb, Figure 2C top left top panel, arrow). The quantitative *p210BCR/ABL* mRNA expression in these samples is shown in Figure S3. As expected from the result of the Northern blot (Figure 2C top left panel), the *p210BCR/ABL* mRNA in the control transgenic spleen was quite low and was significantly enhanced by the transgene integration (nos. 17 and 30). The enhanced expression of p210BCR/ABL at the protein level was confirmed by Western blot using an anti-ABL antibody (Figure 2C bottom left panel).

As for *Zfp423,* no clear message was observed in the control transgenic spleen (Figure 2C top right panel, "C"), which is in accordance with our previous report showing that *Zfp423* message was barely detectable in the spleen when using polyA$^+$ RNA.[34] In contrast, in nos. 18 and 23, an enhanced expression of the *Zfp423* message was observed (~ 6 kb, Figure 2C top right panel, arrow). These results indicated that the retrovirus integrations up-regulated *p210BCR/ABL* expression and induced aberrant *Zfp423* expression.

Expression of *Zfp423* in transgenic BM cells enhanced B-cell colony-forming ability, and suppression of *ZNF423* in *ZNF423*-expressing, *p210BCR/ABL*-positive CML BC cells retarded cell growth

We next investigated the effect of up-regulation and down-regulation of *Zfp423* on the proliferative ability of *p210BCR/ABL*-positive cells. We first examined whether introduction of *Zfp423* confers a growth advantage to transgenic BM cells by a colony formation assay. BM cells purified from wild-type (WT) or *p210BCR/ABL* transgenic mice were infected with control *pMysIG* or *Flag-HA*–tagged *Zfp423 (FHZfp423)*–expressing *pMysIG (pMysIG/FHZfp423)* retrovirus, and the infected cells were cultured in methylcellulose-based media (Figure 3A). Because mice with *Zfp423* activation (nos. 18 and 23) developed B-lineage leukemia, the virus-infected cells were subjected to a B-cell colony assay, and as the retrovirus vector contains *GFP* as a detection marker, colonies with green fluorescence were counted.

The results are shown in Figure 3B. No obvious difference in the colony numbers was found between control *pMysIG* virus-infected WT (WT+control) and *p210BCR/ABL* transgenic (p210BCR/ABL+control) BM cells. This result indicates that the basal *p210BCR/ABL* expression in this transgenic system does not affect the proliferative ability of B cells, probably due to the nature of the promoter used, and is in accordance with our observation that the *p210BCR/ABL* transgenic mice have not developed B-cell disease so far.[14] *pMysIG/FHZfp423*-infected WT BM cells (WT+FHZfp423) showed a slight increase in the colony number in this system. In contrast, *pMysIG/FHZfp423*-infected *p210BCR/ABL* transgenic BM cells (p210BCR/ABL+FHZfp423) generated a significantly increased number of colonies.

We next tried to down-regulate endogenous *ZNF423* (the human homologue of *Zfp423*) by RNA interference and examined its effect on the growth rate. We designed 2 short hairpin RNAs targeted to *ZNF423* mRNA (*shRNA*-1 and *shRNA*-2) and introduced them into BV-173, a *p210BCR/ABL*-positive and *ZNF423*-expressing human hematopoietic cell line (see Figure 5A). As shown in Figure 3C, introduction of *shRNA*-1 effectively decreased

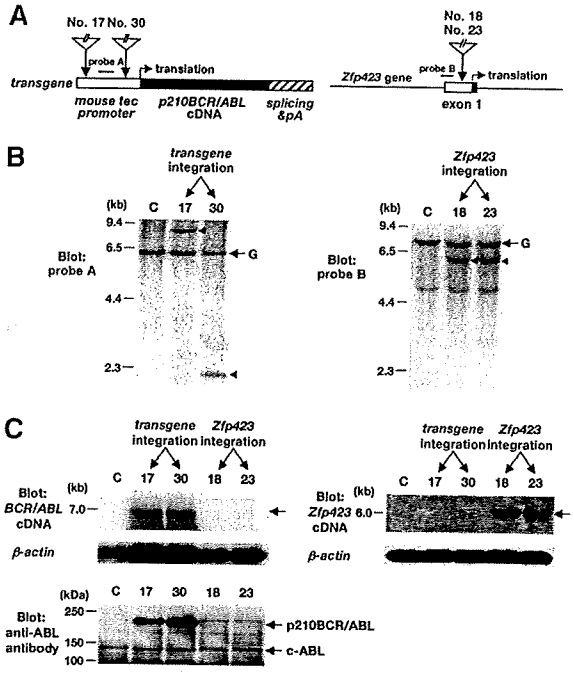

Figure 2. Retrovirus integration sites, genomic rearrangements, and altered gene expressions in mice with B-cell leukemia. (A) Schematic models of retrovirus integration sites. The retrovirus integration sites are indicated by vertical arrows. The left panel illustrates the transgene structure, where the mouse *TEC* promoter, *p210BCR/ABL* cDNA, and polyA and splicing signals are shown by dotted, filled, and shaded boxes, respectively. In mice nos. 17 and 30, retroviruses were integrated approximately 1.5-kb and approximately 200-bp upstream of the transcriptional initiation site, respectively. In the right panel, the noncoding and coding regions of *Zfp423* exon 1 are shown by blank and filled boxes, respectively. In mice nos. 18 and 23, the viral integration occurred almost in the same site, approximately 100-bp upstream of the translational initiation site. The positions of probes used for Southern blots are also shown. (B) Southern blots to confirm the CISs as major integration sites. Genomic DNAs extracted from the spleen of a control transgenic mouse (C) and tumor tissues of the diseased mice (nos. 17, 30, 18, and 23) were digested with *Bam*HI and blotted with a DNA fragment adjacent to the integration site. Probe A (A) was used for transgene rearrangement (nos. 17 and 30, left panel) and probe B was used for *Zfp423* gene rearrangement (nos. 18 and 23, right panel). The positions of germline (G) and rearranged bands are indicated by → and ◄, respectively. Molecular markers are shown on the left. (C) Enhanced expression of *p210BCR/ABL* in mice nos. 17 and 30 and up-regulated expression of *Zfp423* in mice nos. 18 and 23. For detecting *p210BCR/ABL* message, 20 μg total RNAs extracted from the spleen of a control *p210BCR/ABL* transgenic mouse (C) and tumor tissues of the diseased mice (nos. 17, 30, 18, and 23) were blotted with *p210BCR/ABL* cDNA (top left panel) and for detecting *Zfp423* message, 3 μg mRNAs from the same tissues were blotted with a part of *Zfp423* cDNA (top right panel). The result of β-*actin* hybridization is shown as an internal control. Molecular markers are shown on the left and the positions of *p210BCR/ABL* and *Zfp423* messages are indicated by →. Enhanced expression of p210BCR/ABL protein in mice nos. 17 and 30 was detected by blotting the proteins extracted from the same tissues with an anti-ABL antibody (bottom left panel). Protein markers are shown on the left and the positions of p210BCR/ABL and c-ABL (145 kDa) are indicated by →.

ZNF423 mRNA to approximately 40% of that in the parental cells, whereas *shRNA*-2 was less effective. Concurrently, as shown Figure 3D, BV-173 cells transduced with *shRNA*-1 displayed a significantly reduced growth rate, whereas cells expressing *shRNA*-2 showed only marginal growth retardation. To confirm that the *shRNA*s did not affect the growth of cells without *ZNF423* expression, the same *shRNA*s were introduced into KOPN67, a *p210BCR/ABL*-positive but *ZNF423*-nonexpressing cell line (see Figure 5A). As expected, no difference in cell growth was observed in the parental line and *shRNA*s-transduced sublines (Figure S4), confirming the specificity of the *shRNA*s on the *ZNF423*-dependent cell growth. These results indicated that *Zfp423/ZNF423* cooperated with *p210BCR/ABL* and enhanced proliferation of *p210BCR/ABL*-expressing hematopoietic cells.

Zfp423 accelerated disease onset of *p210BCR/ABL*-induced leukemia and increased incidence of B-ALL

We then investigated the in vivo cooperative activity of *Zfp423* and *p210BCR/ABL* by a BMT approach. Because *p210BCR/ABL* transgenic mice were not congenic enough for BMT, we generated *p210BCR/ABL*-expressing retrovirus and *FHZfp423*-expressing retrovirus separately, and infected them with BM cells of Balb/c mice, the strain that has been successfully used to develop CML in the BMT experiments.[10,11] And because *Zfp423*-positive leukemias (nos. 18 and 23) were of B-cell phenotype, BM cells were not pretreated with 5FU and in vitro cultures were performed using a cytokine cocktail with IL-6, IL-3, SCF, and IL-7, as previously described.[11]

BM cells infected with control retrovirus, *p210BCR/ABL*-expressing retrovirus, *FHZfp423*-expressing retrovirus, or both types of viruses were transplanted into sublethally irradiated syngeneic mice (Figure 4A). To detect *p210BCR/ABL*- and *FHZfp423*-positive cells by flow cytometry, cells expressing *p210BCR/ABL* and *FHZfp423* were labeled with *GFP* and *KO* (*Kusabira Orange*),[35] respectively (Figure 4A). The protein expression of the inserted cDNA by retrovirus infection was confirmed by Western blot (Figure S5).

The mice that underwent transplantation were continuously observed and peripheral blood parameters were routinely examined for morphologic changes by Wight-Giemsa staining and for *GFP* and/or *KO* positivities by flow cytometry. The survival rate of each group evaluated using the Kaplan-Meier test is shown in the upper panel of Figure 4B. No disease developed in the control virus-transduced mice. In addition, no hematologic abnormalities were observed in FHZfp423-transduced mice, indicating that overexpression of *Zfp423* does not possess a transforming ability on primary hematopoietic cells, which is in accordance with the result that introduction of *Zfp423* in BM cells did not apparently increase colony numbers (Figure 3B). As expected from the results of previous studies, most of the *p210BCR/ABL*-transduced mice developed CML, except 2 cases that developed acute myeloid leukemia (AML) and B-cell ALL (B-ALL, Figure 4B bottom panel, left bar). In contrast, mice transduced with both types of viruses died in a shortened period and exhibited different phenotypes. The mean survival periods of mice reconstituted with p210BCR/ABL+FHZfp423 and those reconstituted with p210BCR/ABL alone were 29.5 and 48 days, respectively (Figure 4B top panel, thick and thin continuous lines), and the difference was statistically significant ($P < .01$). In addition, compared with mice reconstituted with p210BCR/ABL, those reconstituted with p210BCR/ABL+FHZfp423 exhibited an increased incidence of B-ALL (Figure 5B bottom panel, right bar), although the difference was not statistically significant ($P = .119$), probably due to the limited sample numbers. These results demonstrated that *Zfp423* possesses a cooperative oncogenecity with *p210BCR/ABL* in vivo, which accelerated disease onset and induced a more aggressive phenotype mainly of B-cell lineage. The representative results of pathologic analyses of mice that developed CML by p210BCR/ABL and that developed B-ALL by p210BCR/ABL plus FHZfp423 are shown in Figure 4C and the results of flow cytometry of the latter are shown in Figure 4D. The expression of *p210BCR/ABL* and *Zfp423* mRNAs in tumors developed in p210BCR/ABL plus FHZfp423-transduced mice was confirmed by RT-PCR (Figure S6).

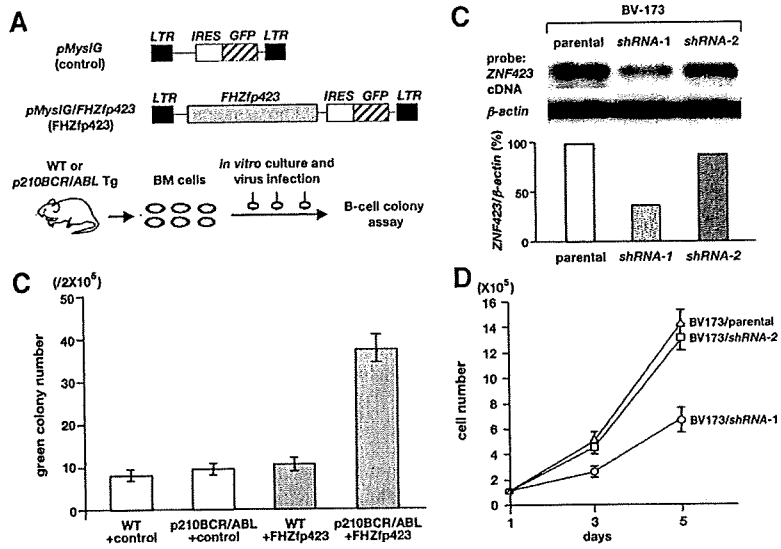

Figure 3. Effects of *Zfp423* expression on the colony formation and proliferation of *p210BCR/ABL*-expressing cells. (A) Schematic structures of the retroviruses and the illustration of the experimental procedure. BM cells were extracted from WT or *p210BCR/ABL* transgenic mice, infected with empty retrovirus (*pMyIG*, control) or *Flag-HA*–tagged *Zfp423 (FHZfp423)*–expressing retrovirus (*pMyIG*/FHZfp423, FHZfp423), and subjected to the B-cell colony assay. (B) Results of B-cell colony assay. The mean green colony number of 3 independent experiments for each group (WT+conrol, p210BCR/ABL+control, WT+FHZfp423, and p210BCR/ABL+FHZfp423) is shown with error bars. (C) Suppression of *ZNF423* expression by *shRNAs*. mRNA (5 μg) extracted from the parental BV-173 line and 2 *shRNA*-introduced sublines (*shRNA-1* and *shRNA-2*) were blotted with a part of the human *ZNF423* coding region. β-*Actin* hybridization was performed as an internal control and the relative expression ratio of *ZNF423* to β-*actin* in each cell line is shown as a vertical column. (D) Results of cell proliferation assay. Cells of the parental BV-173 line and 2 *shRNA*-introduced sublines (BV-173/*shRNA-1* and BV-173/*shRNA-2*) were plated at a density of 10^5/10 cm^2 on day 1 and cell numbers were counted on day 3 and day 5. The mean cell number of 3 independent experiments of each line is plotted with error bars.

Expression of *ZNF423* in human *BCR/ABL*-positive hematopoietic cell lines and CML BC samples

We finally investigated the clinical relevance of *ZNF423* expression in the progression from CML CP to BC using human Ph-positive hematopoietic cell lines and clinical samples. For the cell line experiment, cells expressing *p190BCR/ABL* (an alternative form of the *BCR/ABL* fusion gene) were also examined, because the expression of *p190BCR/ABL* is exclusively associated with B-ALL,[36] the same phenotype as the leukemias developed in the mice with *Zfp423* integration (nos. 18 and 23). In addition, Ph-negative B-ALL lines were included in this study to investigate the role of *ZNF423* in the development of B-cell malignancy without *BCR/ABL*.

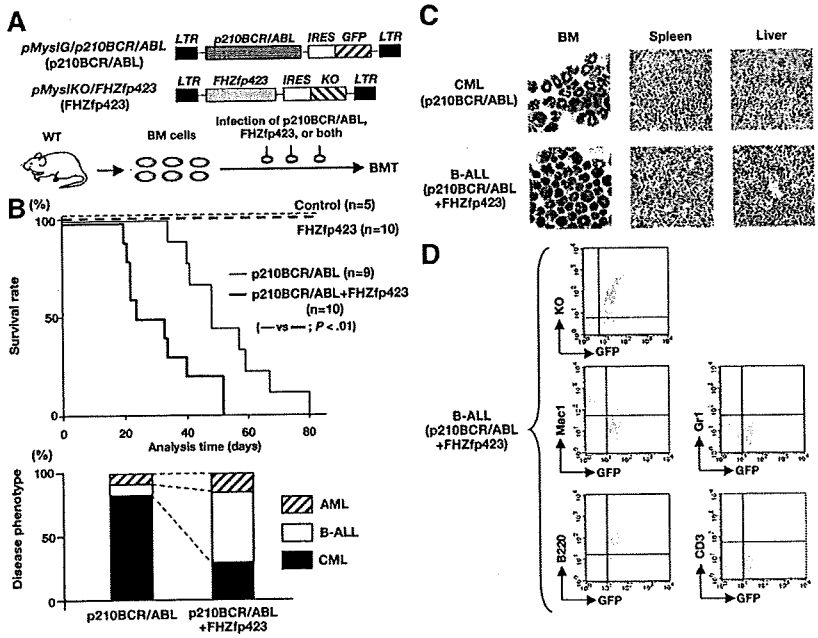

Figure 4. Survival and disease phenotype in mice that received a transplant of *p210BCR/ABL*- and/or *FHZfp423*-expressing BM cells. (A) Schematic structures of the retroviruses and the illustration of the experimental procedure. BM cells infected with *p210BCR/ABL*-expressing retrovirus (*pMyIG/p210BCR/ABL*), *FHZfp423*-expressing retrovirus (*pMyIKO/FHZfp423*), or both types of viruses were subjected to the BMT assay. KO indicates Kusabira Orange. (B) Acceleration of disease onset and altered disease phenotype by cotransduction of *Zfp423* and *p210BCR/ABL*. In the top panel, survival curves of mice reconstituted with BM cells transduced with control retrovirus (control, n = 5), *pMyIKO/FHZfp423* (FHZfp423, n = 10), *pMyIG/p210BCR/ABL* (p210BCR/ABL, n = 9), and both viruses (p210BCR/ABL+FHZfp423, n = 10) are shown as thin dotted, thick dotted, thin continuous, and thick continuous lines, respectively. In the bottom panel, the percentages of samples diagnosed as CML, B-ALL, and AML are shown by black, white, and shaded boxes, respectively. (C) Representative results of pathologic analysis of CML and B-ALL developed in mice transduced with p210BCR/ABL and p210BCR/ABL+FHZfp423, respectively. In the BM smears, proliferation of differentiated myeloid cells is observed in the CML case (top left panel), whereas monotonous proliferation of immature lymphoid tumor cells is apparent in the B-ALL case (bottom left panel). Massive infiltration of leukemic cells is shown in the spleen and liver (middle and right panels). (D) Representative results of flow cytometric analysis of B-ALL developed in mice transduced with p210BCR/ABL and FHZfp423. Leukemic cells are positive for both GFP and KO (top panel), confirming that they were originated from hematopoietic progenitor cells infected with both p210BCR/ABL and FHZfp423. GFP-positive leukemic cells showed positive staining for B220, but are negative for Mac-1, Gr-1, and CD3 (middle and bottom panels).

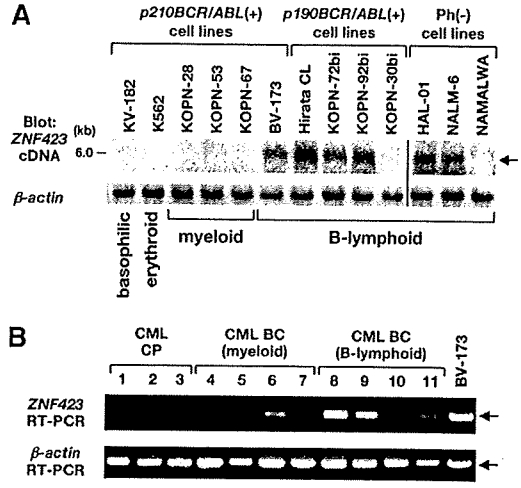

Figure 5. Expression of *ZNF423* in *BCR/ABL*-positive cell lines and in CML BC samples. (A) mRNA (3 μg) extracted from 6 *p210BCR/ABL*-positive, 4 *p190BCR/ABL*-positive, and 3 Ph-negative cell lines was blotted with a part of the human *ZNF423* coding region. β-*Actin* hybridization was performed as an internal control. The position of the *ZNF423* message is indicated by → and the immunophenotypes of the cell lines are shown at the bottom. A vertical line has been inserted to indicate a repositioned gel lane. (B) Total RNAs extracted BM samples from 3 CML CP and 8 CML BC cases (4 myeloid and 4 B-lymphoid) were subjected to RT-PCR for *ZNF423* expression. β-*Actin* RT-PCR was performed as an internal control.

mRNAs extracted from 6 *p210BCR/ABL*-positive cell lines (1 B-lymphoid, 3 myeloid, 1 erythroid, and 1 basophilic), 4 *p190BCR/ABL*-positive B-lymphoid cell lines, and 3 Ph-negative B-lymphoid cell lines were blotted with human *ZNF423* cDNA. As shown in Figure 5A, *ZNF423* mRNA expression was detected in 1 of 6 *p210BCR/ABL*-positive (BV-173), 3 of 4 *p190BCR/ABL*-positive (Hirata CL, KOPN-72bi, and KOPN-92bi), and 2 of 3 Ph-negative cell lines (HAL-01 and NALM-6), all of which were of B-cell phenotype.

We then examined *ZNF423* expression in human clinical samples diagnosed as CML CP or BC. BM samples of 3 CML CP and 4 CML BC patients (4 myeloid and 4 B-lymphoid lineages) with informed consent were subjected to RT-PCR using *ZNF423*-specific primers. BV-173 cells that express *ZNF423* (Figure 5A) were used as a control. As shown in Figure 5B, whereas no *ZNF423* expression was detected in CML CP sample (nos. 1-3), 4 of 8 CML BC samples were found to express *ZNF423*, where 1 was of myeloid (no. 6) and the other 3 were of B-lymphoid (nos. 8, 9, and 11) phenotypes. These results strongly indicated that aberrant expression of *ZNF423* clinically contributes to the malignant transformation of *BCR/ABL*-positive cells and to the progression to CML BC, mainly of B-cell lineage.

Discussion

CML provides an appropriate disease model for multistep carcinogenesis in which generation of p210BCR/ABL initiates CML CP and an additional genetic event(s) contributes to the evolution to CML BC.[8] We developed a transgenic mouse model for human CML, which expresses *p210BCR/ABL* in hematopoietic progenitor cells and reproducibly exhibits a CML-like myeloproliferative disorder.[14] To investigate molecular mechanism(s) responsible for disease progression, the *p210BCR/ABL* transgenic mice were subjected to retroviral insertional mutagenesis. BXH2 mice that harbor a horizontally transmittable replication-competent retrovirus[22] were used as a virus donor strain, because it has been successfully used to detect second hit genes in previous studies.[37-39]

The inbred BXH2 mice were reported to develop acute myeloid leukemia at 7 to 12 months of age due to ecotropic virus integration and intrinsic myeloid tropism.[22-24] In line with this report, all the WT/BXH2 mice died of myeloid leukemia (Figure 1A). In contrast, 6 p210BCR/ABL/BXH2 mice developed nonmyeloid leukemias with a shorter latency. The early disease onset and different phenotypes in these mice indicated that the diseases were caused by the cooperation of *p210BCR/ABL* with altered expression of virus-affected gene(s). Therefore, in this study, we intended to identify virus-integrated genes in the tumors of the 6 mice and iPCR analysis detected 2 CISs in B-cell leukemia samples. These CISs were considered to be strong candidates for CML BC, because leukemia with B-cell phenotype has not been detected in *p210BCR/ABL* transgenic mice[14] and very rarely reported in BXH2 mice (http://rtcgd.abcc.ncifcrf.gov/).[22,23,27]

It is to be noted that one CIS was in the promoter region of the transgene. Interestingly, our previous retrovirus insertional mutagenesis study, in which newborn *p210BCR/ABL* transgenic mice were directly injected with retroviruses, also identified the transgene as a CIS in B-cell BC cases, where retrovirus integration resulted in overexpression and/or enhanced kinase activity of the transgene product.[40] The up-regulation of *p210BCR/ABL* in the blast phase is especially interesting, because it corresponds to double Ph, which is one of the most frequently observed chromosomal abnormalities found in CML BC.[8] Therefore, our observation provides in vivo experimental evidence that acquired enhancement of *p210BCR/ABL* expression accelerates the disease and causes BC. The reason why mice with transgene integration exhibited B-cell leukemia is not clear. It could be possible that *p210BCR/ABL* originally expressed by the *TEC* promoter and then up-regulated by retrovirus insertion might predispose the infected mice to develop B-ALL by an unknown mechanism. In human CML BC, double Ph was reported to be occasionally associated with B-cell BC samples.[41,42]

Another CIS was the 5′ noncoding region of *Zfp423*, which encodes a transcription factor with multiple zinc-finger repeats.[33] Zfp423 was originally identified as a binding partner of Ebf (early B-cell factor, also denoted as Olf1), a protein essential for B-cell and olfactory nervous system development,[43,44] and was subsequently shown to interact with SMADs in response to bone morphogenic protein 2 (BMP2) in the *Xenopus laevis*.[45] *Zfp423* was also cloned as a target in B-cell lymphoma in AKXD27 mice by retroviral insertional mutagenesis.[33] In that study, retrovirus integration occurred upstream of the translation initiation codon resulting in a high level of expression, as observed in our cases (Figure 2).[33] A recent study demonstrated that *Zfp423* knockout mice exhibited abnormal cerebellum development but appeared to have a normal hematopoiesis,[46] suggesting that its ectopic expression would be involved in leukemogenesis.

It remains to be clarified how overexpression of *Zfp423* contributes to B-cell malignancy. Interestingly, although Zfp423 was originally identified as an Ebf-binding partner, it is not expressed in hematopoietic tissues including B cells.[33,34] In the olfactory nervous system, Zfp423 was shown to negatively regulate Ebf function; Zfp423 forms a heterodimer with Ebf, which inhibits Ebf homodimer formation that has an ability to transactivate downstream target genes.[43] Thus, it would be possible that the aberrant expression of *Zfp423* in the hematopoietic system induces B-cell leukemia, at least in part by impairing Ebf-mediated signaling. Alternatively, because a recent study demonstrated that a highly conserved 12–amino acid peptide located in the extreme

N-terminus of Zfp423 recruits the nucleosome remodeling and deacetylase corepressor complex (NuRD),[47] it could be postulated that Zfp423 functions as a transcription repressor and contributes to leukemogenesis by suppressing downstream target genes.

In this study, *Zfp423* was identified as a gene whose deregulated expression cooperates with *p210BCR/ABL* and induces CML BC. The cooperative activities of *Zfp423* and *p210BCR/ABL* were demonstrated by in vitro and in vivo mouse experiments and also by human samples. Enforced expression of *Zfp423* in hematopoietic cells derived from *p210BCR/ABL* transgenic mice enhanced B-cell colony formation, and suppression of *ZNF423* expression in *ZNF423*-expressing, *p210BCR/ABL*-positive CML BC cells reduced cell growth (Figure 3). In addition, expression of *Zfp423* with *p210BCR/ABL* in hematopoietic progenitor cells accelerated *p210BCR/ABL*-mediated leukemia and induced a more aggressive phenotype mainly of B-cell lineage (Figure 4). Furthermore, *ZNF423* is expressed in a subset of *BCR/ABL*-positive hematopoietic cell lines and several CML BC samples mostly with B-cell phenotype (Figure 5). These results demonstrated that *Zfp423/ZNF423* cooperates with *p210BCR/ABL*, confers a proliferative advantage to *p210BCR/ABL*-expressing hematopoietic cells, and consequently develops CML B-cell BC. It is to be noted that *ZNF423* expression was detected in several Ph-negative B-ALL lines (Figure 5), which indicates that *ZNF423* contributes not only to CML B-cell BC or Ph-positive B-ALL but also to de novo B-ALL without *BCR/ABL*.

It is intriguing that while the recipient mice transduced with both *p210BCR/ABL* and *Zfp423* developed mainly B-ALL, 2 cases developed AML (Figure 4B). Although *Zfp423* has been exclusively associated with B-ALL in retroviral insertional mutagenesis studies,[33,34] this result strongly suggests that *Zfp423* might contain a potency to develop AML as well as B-ALL. This idea is in accordance with the finding that one myeloid BC case expressed *ZNF423* in clinical analysis (Figure 5B no. 6). Recently, *Zfp521/ZNF521* (also known as *EHZF [early hematopoietic zinc finger protein]* and *Evi3*), which is homologous to *Zfp423/ZNF423* and was also identified as a target of B-ALLs by mouse retrovirus insertional mutagenesis studies,[34,48] was reported to be frequently involved in AML samples in human leukemias.[49] Thus, a set of zinc finger–containing transcription factors that has been isolated as a target in B-ALL in mice might contribute to leukemias with different phenotypes in humans.

As for the 2 mice that developed T-ALL, although we could not identify any CIS, candidate genes, such as *Hcst (hematopoietic cell signal transducer,* also called *DAP10/KAP10*), an adaptor protein involved in T-cell signaling,[50,51] and *Il21r* (*IL21 receptor*), a cytokine receptor mediating T-cell activation[52,53] were detected (Table S1). In addition, several genes isolated by iPCR have been reported in cancer gene studies. For example, *Avpil1, Ddx6, Runx1, Mef2d, Jak1, Cbfa2t3h,* and *Sox4* have already been identified as retrovirus integration sites in the mouse retrovirus tagged cancer gene database (RTCGD; http://rtcgd.abcc.ncifcrf.gov/),[23,27] and *IL21R, DDx6, Runx1,* and *Cbfa2t3h* have been denoted as chromosomal translocation-associated genes in human cancer (http://www.sanger.ac.uk/genetics/CGP/Census/).[54] Furthermore, *MEF2D* was shown to create a fusion gene in t(1;19)(q23;p13),[55] and *Sox4* was demonstrated to be a powerful tool to identify cooperative genes when transplanted by a replication-defective retrovirus.[56] Further studies will be required to investigate whether virus insertion in these genes might affect the BC phenotype and/or lineage commitment observed in p210BCR/ABL/BXH2 mice.

In this study, we demonstrated that enhanced expression of *p210BCR/ABL* and aberrant expression of *Zfp423/ZNF423* contribute to blastic transformation of *p210BCR/ABL*-expressing hematopoietic cells. Our results provide insights into the molecular mechanism(s) for disease progression of human CML and prove this transgenic system is a valuable tool in identifying genes whose altered expression cooperates with *p210BCR/ABL* to induce CML BC.

Acknowledgments

We thank Yuki Sakai, Kayoko Hashimoto, and Yuko Tsukawaki for the mouse care and technical assistance; Tomoko Takahara and Yukari Yamazaki for BMT studies; and Hirotaka Matsui for the statistical analysis. We also thank Motomi Osato for helpful discussion and Hiroya Aso and Toshiya Inaba for providing us with Ph-positive human hematopoietic cell lines.

This work was supported by a Grant-in-Aid from the Ministry of Education, Science and Culture of Japan (Tokyo, Japan), a Grant-in-Aid for Cancer Research from the Ministry of Health, Labor and Welfare of Japan (13-2; Tokyo, Japan) Research Grant of the Princess Takamatsu Cancer Research Fund (Tokyo, Japan), Mitsubishi Pharma Research Foundation (Osaka, Japan), YASUDA Medical Research Foundation (Osaka, Japan), a Grant-in-Aid of The Japan Medical Association (Tokyo, Japan), and Japan Leukemia Research Fund (Tokyo, Japan).

Authorship

Contribution: K.M., N.Y., M.M., T.N., and H.H. designed and performed the research and wrote the paper; H.O. centralized the pathologic analysis; Y. Komeno, J.K., Z.-i.H., and T. Kitamura, performed the retrovirus and shRNA studies; S.W., N.A.J., and N.G.C. participated in the Zfp423 studies and wrote the paper; T. Kuwata, Y. Kanno, and T.N. contributed to the BMT analysis; and all the authors checked and agreed on the final version of the paper.

Conflict-of-interest disclosure: The authors declare no competing financial interests.

Correspondence: Hiroaki Honda, Department of Developmental Biology, Research Institute of Radiation Biology and Medicine, Hiroshima University, 1-2-3 Kasumi, Minami-ku, Hiroshima 734-8553, Japan; e-mail: hhonda@hiroshima-u.ac.jp.

References

1. Deininger MWN, Goldman JM, Melo JV. The molecular biology of chronic myeloid leukemia. Blood. 2000;96:3343-3356.
2. Ren R. Mechanisms of BCR-ABL in the pathogenesis of chronic myelogenous leukaemia. Nat Rev Cancer. 2005;5:172-183.
3. Rowley JD. A new consistent chromosomal abnormality in chronic myelogenous leukemia identified by quinacrine fluorescence and Giemsa staining. Nature. 1973;243:290-293.
4. de Klein A, van Kessel AG, Grosveld G, et al. A cellular oncogene is translocated to the Philadelphia chromosome in chronic myelocytic leukaemia. Nature. 1982;300:765-767.
5. Groffen J, Stephenson JR, Heisterkamp N, deKlein A, Bartram CR, Grosveld G. Philadelphia chromosomal breakpoints are clustered within a limited region, bcr, on chromosome 22. Cell. 1984;36:93-99.
6. Shtivelman E, Lifshitz B, Gale RP, Canaani E. Fused transcript of abl and bcr genes in chronic myelogenous leukaemia. Nature. 1985;315:550-554.
7. Konopka JB, Watanabe SM, Witte ON. An alternation of the human c-abl protein in K562 leukemia cells unmasks associated tyrosine kinase activity. Cell. 1984;37:1035-1042.

8. Calabretta B, Perrotti D. The biology of CML blast crisis. Blood. 2004;103:4010-4022.
9. Pear WS, Miller JP, Xu L, et al. Efficient and rapid induction of a chronic myelogenous leukemia-like myeloproliferative disease in mice receiving P210 bcr/abl-transduced bone marrow. Blood. 1998;92: 3780-3792.
10. Zhang X, Ren R. Bcr-Abl efficiently induces a myeloproliferative disease and production of excess interleukin-3 and granulocyte-macrophage colony-stimulating factor in mice: a novel model for chronic myelogenous leukemia. Blood. 1998;92:3829-3840.
11. Li S, Ilaria RLJ, Million RP, Daley GQ, Van Etten RA. The P190, P210, and P230 forms of the BCR/ABL oncogene induce a similar chronic myeloid leukemia-like syndrome in mice but have different lymphoid leukemogenic activity. J Exp Med. 1999;189:1399-1342.
12. Honda H, Fujii T, Takatoku M, et al. Expression of p210bcr/abl by metallothionein promoter induced T-cell leukemia in transgenic mice. Blood. 1995; 85:2853-2861.
13. Voncken JW, Kaartinen V, Pattengale PK, Germeraad WTV, Groffen J, Heisterkamp N. BCR/ABL p210 and p190 cause distinct leukemia in transgenic mice. Blood. 1995;86:4603-4611.
14. Honda H, Oda H, Suzuki T, et al. Development of acute lymphoblastic leukemia and myeloproliferative disorder in transgenic mice expressing p210bcr/abl: a novel transgenic model for human Ph1-positive leukemias. Blood. 1998;91:2067-2075.
15. Huettner CS, Zhang P, Van Etten RA, Tenen DG. Reversibility of acute B-cell leukaemia induced by BCR-ABL1. Nat Genet. 2000;24:57-60.
16. Huettner CS, Koschmieder S, Iwasaki H, et al. Inducible expression of BCR/ABL using human CD34 regulatory elements results in a megakaryocytic myeloproliferative syndrome. Blood. 2003;102:3363-3370.
17. Koschmieder S, Gottgens B, Zhang P, et al. Inducible chronic phase of myeloid leukemia with expansion of hematopoietic stem cells in a transgenic model of BCR-ABL leukemogenesis. Blood. 2005;105:324-334.
18. Honda H, Yamashita Y, Ozawa K, HM. Cloning and characterization of mouse tec promoter. Biochem Biophys Res Commun. 1996;223:422-426.
19. Honda H, Ozawa K, Yazaki Y, Hirai H. Identification of PU. 1 and Sp1 as essential transcriptional factors for the promoter activity of mouse tec gene. Biochem Biophys Res Comm. 1997;234: 376-381.
20. Honda H, Ushijima T, Wakazono K, et al. Acquired loss of p53 induces blastic transformation in p210bcr/abl-expressing hematopoietic cells: a transgenic study for blast crisis of human CML. Blood. 2000;95:1144-1150.
21. Niki M, Cristofano DA, Zhao M, et al. Role of Dok-1 and Dok-2 in leukemia suppression. J Exp Med. 2004;200:1689-1695.
22. Li J, Shen H, Himmel KL, et al. Leukaemia disease genes: large-scale cloning and pathway predictions. Nat Genet. 1999;23:348-353.
23. Akagi K, Suzuki T, Stephens RM, Jenkins NA, Copeland NG. RTCGD: retroviral tagged cancer gene database. Nucleic Acids Res. 2004;32(database issue):D523-D527.
24. Turcotte K, Gauthier S, Tuite A, Mullick A, Malo D, Gros P. A mutation in the Icsbp1 gene causes susceptibility to infection and a chronic myeloid leukemia-like syndrome in BXH-2 mice. J Exp Med. 2005;201:881-890.
25. Miyazaki K, Kawamoto T, Tanimoto K, Nishiyama M, Honda H, Kato Y. Identification of functional hypoxia response elements in the promoter region of the DEC1 and DEC2 genes. J Biol Chem. 2002;277:47014-47021.
26. University of Colombo School of Computing. UCSC Genome Browser. http://genome.ucsc.edu. Accessed January 2009.
27. National Cancer Institute–Frederick. Mouse Retrovirus Tagged Cancer Gene Database. http://rtcgd.abcc.ncifcrf.gov. Accessed January 2009.
28. Kitamura T, Koshino Y, Shibata F, et al. Retrovirus-mediated gene transfer and expression cloning: powerful tools in functional genomics. Exp Hematol. 2003;31:1007-1014.
29. Morita S, Kojima T, Kitamura T. Plat-E: an efficient and stable system for transient packaging of retroviruses. Gene Ther. 2000;7:1063-1066.
30. Jin G, Yamazaki Y, Takuwa M, et al. Trib1 and Evi1 cooperate with Hoxa and Meis1 in myeloid leukemogenesis. Blood. 2007;109:3998-4005.
31. Kono H, Kyogoku C, Suzuki T, et al. FcgammaRIIB Ile232Thr transmembrane polymorphism associated with human systemic lupus erythematosus decreases affinity to lipid rafts and attenuates inhibitory effects on B cell receptor signaling. Hum Mol Genet. 2005;14:2881-2892.
32. Harada H, Harada Y, Tanaka H, Kimura A, Inaba T. Implications of somatic mutations in the AML1 gene in radiation-associated and therapy-related myelodysplastic syndrome/acute myeloid leukemia. Blood. 2003;101:673-680.
33. Warming S, Suzuki T, Yamaguchi TP, Jenkins NA, Copeland NG. Early B-cell factor-associated zinc-finger gene is a frequent target of retroviral integration in murine B-cell lymphomas. Oncogene. 2004;23:2727-2731.
34. Warming S, Liu P, Suzuki T, et al. Evi3, a common retroviral integration site in murine B-cell lymphoma, encodes an EBFAZ-related Kruppel-like zinc finger protein. Blood. 2003;101:1934-1940.
35. Sanuki S, Hamanaka S, Kaneko S, et al. A new red fluorescent protein that allows efficient marking of murine hematopoietic stem cells. J Gene Med. 2008;10:965-971.
36. Pane F, Intrieri M, Quintarelli C, Izzo B, Muccioli GC, Salvatore F. BCR/ABL genes and leukemic phenotype: from molecular mechanisms to clinical correlations. Oncogene. 2002;21:8652-8667.
37. Iwasaki M, Kuwata T, Yamazaki Y, et al. Identification of cooperative genes for NUP98-HOXA9 in myeloid leukemogenesis using a mouse model. Blood. 2005;105:784-793.
38. Yanagida M, Osato M, Yamashita N, et al. Increased dosage of Runx1/AML1 acts as a positive modulator of myeloid leukemogenesis in BXH2 mice. Oncogene. 2005;24:4477-4485.
39. Yamashita N, Osato M, Huang L, et al. Haploinsufficiency of Runx1/AML1 promotes myeloid features and leukaemogenesis in BXH2 mice. Br J Haematol. 2005;131:495-507.
40. Mizuno T, Yamasaki N, Miyazaki K, et al. Overexpression/enhanced kinase activity of BCR/ABL and altered expression of Notch1 induced acute leukemia in p210BCR/ABL transgenic mice. Oncogene. 2008;27:3465-3474.
41. Tien HF, Chuang SM, Wang CH, et al. Chromosomal characteristics of Ph-positive chronic myelogenous leukemia in transformation: a study of 23 Chinese patients in Taiwan. Cancer Genet Cytogenet. 1989;39:89-97.
42. Griesshammer M, Heinze B, Bangerter M, Heimpel H, Fliedner TM. Karyotype abnormalities and their clinical significance in blast crisis of chronic myeloid leukemia. J Mol Med. 1997;75: 836-838.
43. Tsai RY, Reed RR. Cloning and functional characterization of Roaz, a zinc finger protein that interacts with O/E-1 to regulate gene expression: implications for olfactory neuronal development. J Neurosci. 1997;17:4159-4169.
44. Tsai RY, Reed RR. Identification of DNA recognition sequences and protein interaction domains of the multiple-Zn-finger protein Roaz. Mol Cell Biol. 1998;18:6447-6456.
45. Hata A, Seoane J, Lagna G, Montalvo E, Hemmati-Brivanlou A, Massague J. OAZ uses distinct DNA- and protein-binding zinc fingers in separate BMP-Smad and Olf signaling pathways. Cell. 2000;100:229-240.
46. Warming S, Rachel RA, Jenkins NA, Copeland NG. Zfp423 is required for normal cerebellar development. Mol Cell Biol. 2006;26: 6913-6922.
47. Lauberth SM, Rauchman MA. Conserved 12-amino acid motif in Sall1 recruits the nucleosome remodeling and deacetylase corepressor complex. J Biol Chem. 2006;281:23922-23931.
48. Hentges KE, Weiser KC, Schountz T, Woodward LS, Morse HC, Justice MJ. Evi3, a zinc-finger protein related to EBFAZ, regulates EBF activity in B-cell leukemia. Oncogene. 2005; 24:1220-1230.
49. Bond HM, Mesuraca M, Amodio N, et al. Early hematopoietic zinc finger protein-zinc finger protein 521: a candidate regulator of diverse immature cells. Int J Biochem Cell Biol. 2008;40:848-854.
50. Wu J, Song Y, Bakker AB, et al. An activating immunoreceptor complex formed by NKG2D and DAP10. Science. 1999;285:730-732.
51. Chang C, Dietrich J, Harpur AG, et al. Cutting edge: KAP10, a novel transmembrane adapter protein genetically linked to DAP12 but with unique signaling properties. J Immunol. 1999; 163:4651-4654.
52. Mehta DS, Wurster AL, Grusby MJ. Biology of IL-21 and the IL-21 receptor. Immunol Rev. 2004; 202:84-95.
53. Leonard WJ, Spolski R. Interleukin-21: a modulator of lymphoid proliferation, apoptosis and differentiation. Nat Rev Immunol. 2005;5:688-698.
54. Wellcome Trust Sanger. Cancer Gene Census. http://www.sanger.ac.uk/genetics/CGP/Census. Accessed _.
55. Yuki Y, Imoto I, Imaizumi M, et al. Identification of a novel fusion gene in a pre-B acute lymphoblastic leukemia with t(1;19)(q23;p13). Cancer Sci. 2004;95:503-507.
56. Du Y, Spence SE, Jenkins NA, Copeland NG. Cooperating cancer-gene identification through oncogenic-retrovirus-induced insertional mutagenesis. Blood. 2005;106:2498-2505.